Summer 2012

NIH Shift Literature Search

Nicole Owens
Governors State University

NIH SHIFT LITERATURE RESEARCH

BY: NICOLE OWENS

UNDER THE DIRECTION

OF DR. S. KUMAR AT

GOVERNORS STATE UNIVERSITY

IN UNIVERSITY PARK ILLINOIS

May 1, 2012

Introduction:

The NIH shift or the National Institute of health shift gets its name from the founders of this mechanism. The National Institute of Health was the first to observe this phenomenon in there studies and are the first to report this chemical shift. The NIH shift is a chemical shift of substituents in aromatic hydroxylation reactions. The substituents that undergo this shift are hydrogen, halogens, acyl and alkyl groups. It is an important aspect that is a requirement in the hydroxylation of aromatic compounds by monooxygenase enzymes. In the hydroxylation of aromatic compounds the substituents undergo a 1, 2 migration reaction also known as the NIH shift. The transfer of an oxygen atom in the monooxygenase enzyme catalyzed reaction is electrophilic, and the substituents that participate in this mechanism activate the aromatic ring to an electrophilic attack. Deactivating groups consist of electron withdrawing groups that activate the aromatic ring towards an electrophilic attack. These groups are attached to a ring and this allows for the removal of electron density from the ring. These groups are classified as weak, moderate, and strong deactivating groups. The weak deactivating groups direct the electrophiles to attack the benzene molecule at the ortho and the para positions on the ring. On the other hand, strongly and moderately deactivating groups direct attacks to the meta position of the aromatic ring. Dr. Kumar has shown an acyl migration in an intramolecular NIH shift study at Governors State University. In this literature search I have examine the NIH shift in different aspects in order to build on and give insight into Dr. Kumar's study on the NIH shift and its mechanism in the hydroxylation reactions. This mechanism is apparent in the pterin dependent amino acid hydroxylases that include tyrosine, tryptophan, and phenylalanine. The reaction is also

apparent in the metal centered oxygen atom transfer to organic substrates. In this report the NIH shift and hydroxylation reactions will be studied and reported in depth. I began my literature search in the years following Dr. Kumar's research on the subject. Hydroxylation is a chemical process that introduces a hydroxyl group into an organic compound. Hydroxylation is the first step in the oxidative degradation of organic compounds in air. It is extremely important in detoxification since hydroxylation converts lipophilic compounds into hydrophilic products that are more readily excreted, and some drugs are activated or deactivated by hydroxylation. Hydroxylases are any of a group of enzymes that catalyze the formation of a hydroxyl group on a substrate by incorporation of one atom or two atoms of oxygen from dioxygen. They all are homotetrameric, contain a mononuclear iron and utilize dioxygen and tetrahydrobiopterin as substrates in a hydroxylase reaction. In this literature search I have surveyed a number of hydroxylation reactions that the NIH shift plays an important role in using various physiological and non physiological substrates. Synthesis of compounds used for further examination is empirical to the understanding of the mechanisms involved, and is important in most hydroxylation reactions.

Article #1

A Mechanism for Hydroxylation by Tyrosine Hydroxylase Based on Partitioning of Substituted Phenylalanines

Summary:

Tyrosine hydroxylase is an enzyme that catalyzes the reaction of tyrosine to 5-dihydroxyphenylalanine. In this study the authors propose a mechanism to better understand the reactions catalyzed by this enzyme. This enzyme is one of three pterin-

dependent amino acid hydroxylases that contain iron. There is not a wealth of information available about the chemistry of this family of enzymes, although previously published literature suggest that the rate limiting step forms an intermediate, followed by rapid hydroxylation of the amino acid. This study focuses on events that happen following the formation of the hydroxylating intermediate, using five substituted phenylalanines as substrates to provide insight into tyrosine hydroxylases chemical mechanism. The materials used in this study include tyrosine, phenylalanine, 4-aminophenylalanine, 4-methoxyphenylalanine, 4-fluorophenylalanine, 4-chlorophenylalanine, 4-bromophenylalanine, 3-chlorotyrosine, 3-iodotyrosine, sheep liver dihydropteridine reductase, and NADH were all bought from Sigma chemical company. The 4-methoxyphenylalanine, 3-chlorotyrosine, and 3-iodotyrosine were purified using HPLC and 3-Fluorotyrosine, 3-mercaptopropionic acid, and all chemicals used for organic synthesis were bought from Aldrich chemical company. M-tyrosine was bought from Lancaster Synthesis, and o-phthalaldehyde was obtained from Aldrich chemical company and tetrahydrobiopterin was obtained from Fluka chemical company. The compound 6-methyltetrahydropterin was synthesized, and recombinant rat tyrosine hydroxylase was purified according to previous studies. There were various analytical methods used in this study including; UV/VIS spectra, HPLC and derivatized products were detected by fluorescence spectroscopy. The results of this study are reported in terms of the kinetic parameters using Km and Vmax values for the substrates, the product formation from the substituted phenylalanines, and the stoichiometry of the hydroxylation reactions.

Table 1: Apparent Steady-State Kinetic Parameters for Alternate Substrates of Tyrosine Hydroxylase at pH 7.1 and 25 °C[a]

substrate	K_m (μM)	V_{max} (min^{-1})
phenylalanine	41.6 ± 9.1	16.9 ± 1.2
tyrosine	4.9 ± 1.9	36.9 ± 4.1
4-methoxyphenylalanine	1350 ± 290	20.0 ± 2.2
4-methylphenylalanine	1100 ± 200	19.3 ± 1.9
4-fluorophenylalanine	110 ± 20	48.2 ± 4.3
4-chlorophenylalanine	220 ± 50	13.8 ± 1.1
4-bromophenylalanine	240 ± 60	9.2 ± 0.9

[a] Initial velocities were determined by following the rate of dihydropterin production with variable amounts of amino acid, 10 μM 6-methyltetrahydropterin, and 0.6 unit/mL sheep dihydropterin reductase, 200 μM NADH, 100 μg/mL catalase, 0.25 μM tyrosine hydroxylase, and 50 mM HEPES (pH 7.1) in a volume of 0.7 mL at 25 °C.

Table # 1 above provides the kinetic parameters of the substituted phenylalanines, tyrosine, and phenylalanine examined in this study. The information in this study is consistent with other studies using similar enzymes. There is an increase in the Km values over the range of the five 4-X-substituted phenylalanines with the heavier substituent showing the largest Km value of 1350 (=/-) 290 for the methoxy substrate and the smaller substituent showing the lowest value of Km. The Vmax values range from 9.2 to 48.2 for the five substituents used. In contrast to previous studies involving the rat and bovine enzymes the small change in Vmax values suggest that there was a slow catalysis mechanism that doesn't involve the amino acid. The kinetic parameters in this table suggest that all five amino acids are substrates for tyrosine hydroxylase. The products formed from 4-chlorophenylalnine and 4-fluorophenylalanine, were determined using HPLC and reported in table #2.

Figure #1 below shows the chromatograph of the products formed from 4-chlorophenylalnine graph (B) and 4-fluorophenylalanine graph (A). From the graph and data points dopa formation is apparent on both graphs as seen from the dark circular data points. Graph (A) shows dopa formation at lower but increasing concentrations with time. Tyrosine shown by the triangular points increases with time and higher concentrations than dopa. Graph (B) also shows an increase in dopa concentration over time with the hydroxyphenalanine component also increasing with higher concentration than dopa over

time. Both graphs prove that dopa formation from the two previously mentioned substrates is possible.

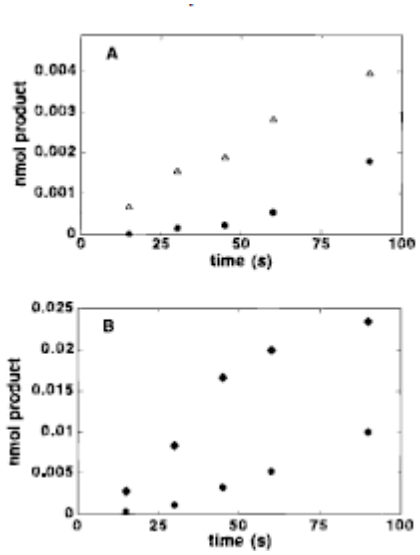

Scheme #2 gives an explanation of the possible routes of dopa formation in this reaction. Pathways 1 and 2 can occur with hydroxylation of the initial halogenated already hydroxylated product, while pathway 3 is achieved with further hydroxylation of tyrosine. In pathway 5 and pathway 4 using the halogenated substituents on the 4th carbon site (4-chlro, 4-bromo-3-hydroxyphenylalanine) the only amino acid product formed is dopa, but when the halogenated substituent is on the 3rd carbon (3-chloro and, 3-bromo-4-hydroxyphenylalanine) and are used as substrates for the enzyme, there was no dopa formed.

Scheme 2

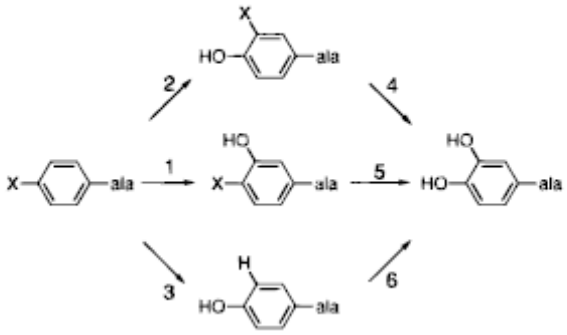

Table #2 gives a summary of the many products formed for the 4-substituted phenylalanine substrates used in this study and it provides the product distribution showing variations in the sites of hydroxylation with the five different substrates. The table reports the values in terms of the percent of formation, the percent of substrate coupling, the NIH shift and para versus meta addition in the products formed. There are several products formed for the five substrates studied. When 4-bromophenylalanine (pathways 1-3) shows the three resultant products, when 4-methylphenylalanine is used (pathways 1and 2) gives the products, and when 4-chlorophenylalanine are used three products results from each of these reactions. Consequently, pathway (1) shows 4-methoxy-3-hydroxyphenalanine is the only product formed when 4-methoxyphenylalanine is used as a substituent. Tyrosine is the only product from the reaction of 4-fluorophenylalanine. Table #2 summarizes the coupling values obtained for the five substrates used in this study. There is a wide range of coupling values that suggest smaller values when the halogen substituents are used and larger values with the methyl and methoxy substituents.

Figure #2 below provides a graphical scheme of the effects of the Van der Waals volume of the C-4/3 group of the substituent versus the position of attack. The graph provides

information suggesting the bigger size substituents at the 4th position prefer hydroxylation at the 3rd position of the aromatic ring. The percent of attack for the heaviest methoxy compound at the 4th position is zero percent on the graph but the percentage of hydroxylation on the 3rd position is approximately 100% supporting the analogy that the larger substituents prefer hydroxylation at the 3rd position oppose to the 4th position on the ring. The smaller percentages are seen when hydroxylation favors the C-4 position for the smaller hydrogen and fluorine substituents. Higher percentages of about 40-50% are seen when chlorine, bromine, and the methyl groups are used directing the attack on the 3rd position of the ring.

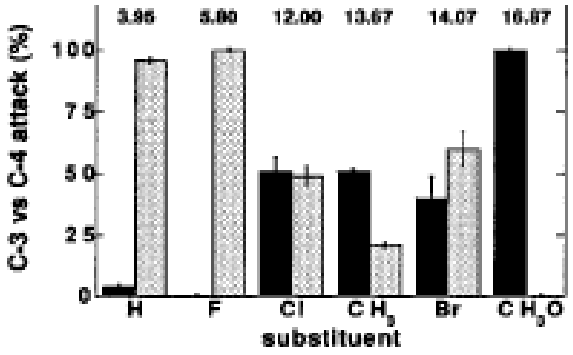

Table # 3 below presents a summary of the Hammett Constants from the coupling for the substrates used. The roe values are consistent with the formation of a cationic intermediate, which means there is a highly electron deficient transition state for the hydroxylation reaction. The correlation values are between 91-98% showing a very good correlation between the data. The roe values should be close to -5 for the cationic intermediate to be present and the 6MPH4 coupling roe values range from (~-3.3 to ~-5.6) and the BH4 values range from ~(-2.4 to~-4.3). These values are consistent with a cationic intermediates presence.

Table 3: Hammett Constants Determined from Coupling for Substrates of Tyrosine Hydroxylase[a]

	BH_4		$6MPH_4$	
	ρ	R	ρ	R^b
σ	-4.3 ± 0.7	0.95	-5.6 ± 0.8	0.96
σ^+	-4.6 ± 0.4	0.98	-5.9 ± 0.8	0.97
σ^-	-2.4 ± 0.5	0.91	-3.3 ± 0.4	0.97

[a] ρ values determined from coupling values from Table 2 for amino acid substrates using the equation $-\log(1/C-1)$, where C is the coupling. [b] R is the correlation coefficient from the fit of the data to the equation $-\log(1/C-1) = \rho\sigma + b$.

The authors in this study examine several mechanisms for analyzing the partitioning of alternate substrates among multiple products. The results shown here provide new information into the mechanism of tyrosine hydroxylase. Different hydroxylated products can form from a single substrate and the products result once formation of the hydroxylating intermediate occurs. Sterics are important in these hydroxylation reactions because the size of the substituent at the C-4 position is a determinant of the site of hydroxylation, with hydroxylation occurring on the C-3 position when the substituents size is large. The data shows high values of the NIH shift for hydrogen and bromine substituents and smaller values with chlorine and methylated substituents. The NIH shift values listed as zero in table #2 for methoxy and fluorine substituents. This information proves the NIH shift is seen with functional groups in a pattern consistent with the presence of a cationic intermediate. This study shows a mechanism of oxygen incorporation into the $3^{rd}/4^{th}$ position on the aromatic ring, causing the ring to become electrophilic, which can then causes the ring to undergo a NIH shift. The hydroxylating product is then produced after rearomatization of the ring is achieved. In future studies the authors can use moderately deactivating groups to probe the interactions of this enzyme that is very important for scientific studies.

Article: #2

Title: Hydroxylation and Methylthiolation of Mono-Ortho-Substituted Polychlorinated Biphenyls in Rats: Identification of Metabolites with Tissue Affinity

Summary:

Polychlorinated biphenyls are toxic manmade organic compounds that contain up to ten chlorine atoms attached to two phenyl groups. This chemical can exhibit a wide range of toxic effects in animals and are known environmental pollutants. PCBs can be transported long distances thru there binding strength to soil and sediment, and are found in the air and water. These toxic PCB's are reported to accumulate in human milk and adipose tissue and are involved in producing methylthio metabolites. The authors in this study choose to examine the metabolism of three polychlorinated biphenyls: (CB105), (CB118), (CB156). These toxic PCB's are reported to accumulate in human milk and adipose tissue and are involved in producing methylthio metabolites. This article investigates the three mono/ortho-substituted polychlorinated biphenyls with inferences on there tissue retention in rats and the identification of methylthio and hydroxy metabolites. There are two internal standards used for this study; 4′-methyl-3′-MeSO2-2,3,4,5,5′-pentaCB and 2,3,3′,4,4′,5,5′-heptaCB. The four reference compounds were synthesized according to the procedures in this article; 5-MeSO2-2,3,3′,4,4′-pentaCB, 5′-MeSO2-2,3,3′,4,4′-pentaCB, 5′-MeSO2-2,3′,4,4′,5-pentaCB, and 5′-MeSO2-2,3,3′,4,4′,5-hexaCB and the methoxy derivatives that were used for identification purposes were obtained and synthesized. There are three mono-ortho substituted congeners used in this article they are; 2,3,3′,4,4′-pentachlorobiphenyl (CB105), 2,3′,4,4′,5-pentachlorobiphenyl (CB118), and 2,3,3′,4,4′,5-hexachlorobiphenyl (CB156). Male Wister rats weighing

approximately 200 g were treated in a controlled environment and their fecal excretions were collected for analysis. The rats were then killed after four days and their organs were removed for further analysis of the metabolites. Isolation of the metabolites was then achieved using previous sample cleanup and quantification methods. Three analytical methods were used in this article; proton NMR, GC/MS, and GC/ECD. The samples were dissolved in chloroform and analyzed using proton NMR. The metabolites were quantified using GC/MS, the samples were identified using GC/MS and compared with known synthesized metabolites. The results are discussed in terms of the identification of fecal metabolites, excretion rate and tissue distribution of the metabolites studied using the gas chromatograph. Figure #1 contains two chromatograms of the fecal extracts obtained from the Wister rats treated with CB105. Graph A contains the acidic fraction from the feces showing five peaks identifying five separate compounds. The five peaks are identified by there retention times after comparison to known compounds. The acidic chromatogram (1a) contained five methoxy metabolites that were identified as 4-MeO 2,3,3',4'-tetraCB, 5-MeO-2,3,3',4,4'-pentaCB, 5'-MeO- 2,3,3',4,4'-pentaCB, 4'-MeO-2,3,3',4,5'-pentaCB and 4-MeO-2,3,3',4',5-pentaCB. The neutral fraction shows four peaks identified as CB105 and methylsulfonyl metabolites. The resultant methylsulfonyl metabolites were identified as CB105 6'-MeSO2 CB105, 6-MeSO2-CB105, 5-MeSO2 CB105, and 5'-MeSO2 CB-105.

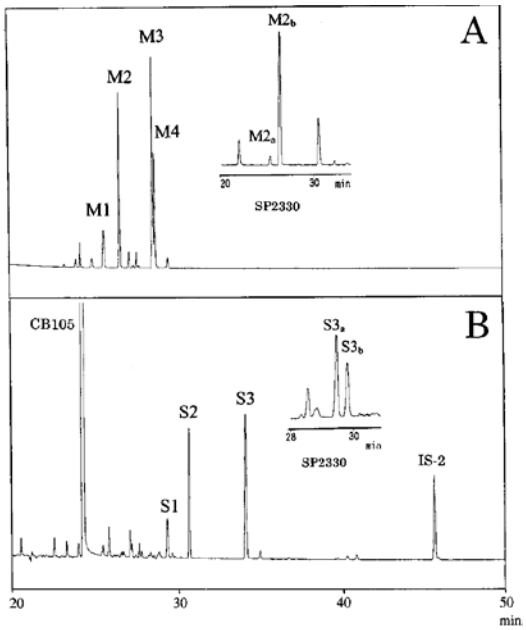

Figure # 2 is a total ion chromatogram of the neutral sample after oxidation of this fraction. There are four peaks in the chromatogram and are identified as the same compounds previously listed above, noting that the first identification is accurate. The graphs show peaks at 402 m/z for all four compounds in the mass spectra below.

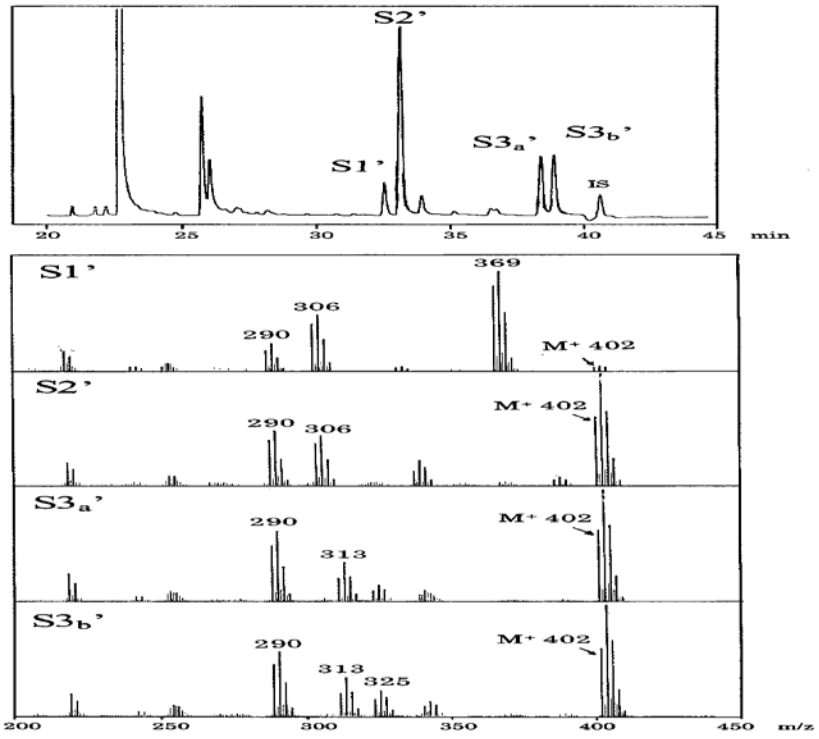

Table #1 below contains the mass spectral summary of the methylsulfonyl metabolites that result from the feces of the rats tested in this study. The S1 peak shows an 80% relative abundance for the M+-50 peak, and S2 has a 58% relative abundance fragment ion for the M+-50 this means the there is an ortho-methylthio substituted cogener present. There is a fragment ion in the S1 peak with a relative abundance of 80% for the M+-35 ion that is characteristic of an ortho-chlorine atom on the ring opposite the methylsulfonyl group. The S3 peak was further separated into two on a different column due to the coelution on the 1st column, and the peaks show the M+-33 fragment ion which is indicative of a meta or para methylthio substituted cogener. The S4 peak has a 80% relative abundance fragment ion at M+-35 showing ortho-methylsulfonyl substitution, while the S5 peak gave a 8% relative abundance ion at M+-33 although this is low it indicates the presence of a meta or para methylsulfonyl substitution. The S6 peak shows a M+-35 peak with a relative abundance of 55% showing a ortho-methylthio substitution

and S7 shows a M+-33 ion indicating a meta or para methylthio substitution.

Figure # 3 provides the chromatogram of the fecal extracts taken from the CB118 treated rats. There is an acidic and neutral fraction in figure # 3 the acidic graph (a) has four peaks while the neutral fraction has five peaks with two of the peaks being the internal standards peaks. The four peaks are identified as monohydroxy metabolites and there methylated derivatives. The compounds are 4-MeO-2, 3′, 4′, 5-tetraCB, 4′-MeO-2, 3′, 4, 5, 5′-pentaCB, 4-MeO-2, 3, 3′, 4′, 5-pentaCB, and 5′MeO-CB118. In figure 3b the three peaks were identified as unchanged CB118 and two methylthio metabolites, 6′-MeS-CB118 and 5′-MeS-CB118.

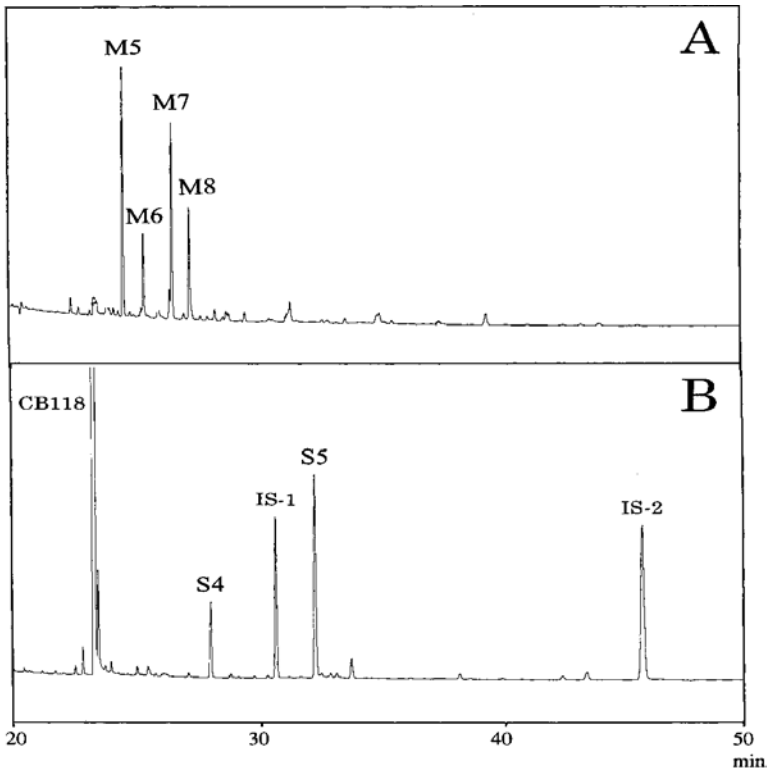

Figure # 4 above shows the chromatograms for the CB156 treated rat fecal excretions where the acidic fraction of the CB156 treated feces shows two hydroxyl metabolites and there methylated derivatives. Figure (a) shows two peaks that have been identified as 4′-

MeO-2, 3, 3′, 4, 5, 5′-hexaCB and 5′-MeO-CB156. Figure (b) the neutral fraction has three peaks identified as CB156 and 6′-MeS-CB156 and 5′-MeS-CB156.

Table #2 below provides a summary of the results of the excretion rate of the metabolites in percentages. The rats treated with CB105 excreted 2.2% as five hydroxyl metabolites, and 0.2% was excreted as four methylthio metabolites. The rats treated with CB118 excreted 1.9% as four hydroxyl metabolites while only 0.16% is excreted as two methylthio metabolites. The CB156 treated rats excreted 0.08% as two hydroxyl metabolites and less than 0.01% of the dose was reported as two methylthio metabolites.

Table 2. Fecal Excretion of Unchanged CB and Hydroxy and MeS Metabolites in Rats to Which Three Mono-Ortho-PCBs Were Administered[a]

	extent of excretion (% dose)				
PCB congener	unchanged CB	hydroxy metabolites	ratio of hydroxy metabolites identified	MeS metabolites	ratio of MeS metabolites identified
CB105	1.2	2.2	7:3:2:2:1 4-OH-2,3,3′,4′,5-pentaCB: 5′-OH-CB105:5-OH-CB105: 4-OH-2,3,3′,4′-tetraCB:4′-OH-2,3,3′,4,5′-pentaCB	0.20	5:2:2:1 6-MeS-CB105: 5-MeS-CB105: 5′-MeS-CB105: 6′-MeS-CB105
CB118	0.9	1.9	12:4:1:1 4-OH-2,3′,4′,5-tetraCB: 4-OH-2,3,3′,4′,5-pentaCB: 4′-OH-2,3′,4,5,5′-pentaCB:5′-OH-CB118	0.16	4:1 5′-MeS-CB118: 6′-MeS-CB118
CB156	0.7	0.08	3:1 4′-OH-2,3,3′,4,5,5′-hexaCB:5′-OH-CB156	<0.01	3:1 5′-MeS-CB156: 6′-MeS-CB156

[a] Values represent the means of the accumulated extents of excretion for four rats during the first 4 days after PCB treatment.

Table #3 below provides the concentration of unchanged CB, methylthio, and hydroxyl metabolites in the blood and tissue of Wister rats.CB105 treated rats show a single hydroxyl metabolite detected in the blood and the liver and adipose tissue. The metabolites concentration in the blood of the treated rats is 3 times higher than the other tissues investigated. There were two methylsulfonyl metabolites detected in the liver and the adipose tissue. CB118 treated rats had two hydroxyl metabolites that were retained in the blood and liver. Methylsulfonyl metabolites were only retained in the liver with the CB118 treated rats. CB156 treated rats retained one hydroxyl metabolite in blood and all tissues tested.

Table 3. Blood and Tissue Concentrations of Unchanged CB and Hydroxy and $MeSO_2$ Metabolites in Rats to Which Three Mono-Ortho-PCB Congeners Were Administered[a]

	blood and tissue concentration (nmol/g wet weight)				
	blood	liver	lung	kidney	adipose tissue
CB105					
unchanged CB	0.22 ± 0.02	9.50 ± 0.77	7.85 ± 0.55	4.66 ± 0.73	373 ± 137
4-OH-2,3,3′,4′,5-pentaCB	2.47 ± 0.05	0.71 ± 0.18	0.82 ± 0.20	0.59 ± 0.11	0.37 ± 0.08
5′-$MeSO_2$-CB105	ND[b]	0.021 ± 0.003	<0.001	<0.001	0.07 ± 0.01
6′-$MeSO_2$-CB105	ND	0.004 ± 0.001	<0.001	0.004 ± 0.001	0.38 ± 0.07
CB118					
unchanged CB	0.21 ± 0.10	11.1 ± 2.06	4.33 ± 0.56	3.85 ± 0.63	181 ± 64.2
4-OH-2,3,3′,4′,5-pentaCB	1.55 ± 0.14	0.51 ± 0.04	0.41 ± 0.05	0.31 ± 0.07	0.22 ± 0.05
4′-OH-2,3′,4,5,5′-pentaCB	0.35 ± 0.07	0.08 ± 0.01	0.09 ± 0.02	0.07 ± 0.01	ND
5′-$MeSO_2$-CB118	ND	0.072 ± 0.02	0.006 ± 0.001	0.005 ± 0.001	0.05 ± 0.01
6′-$MeSO_2$-CB118	ND	0.004 ± 0.001	0.009 ± 0.002	0.005 ± 0.001	0.03 ± 0.01
CB156					
unchanged CB	0.54 ± 0.07	11.7 ± 3.27	6.88 ± 0.97	8.84 ± 1.42	416 ± 129
4′-OH-2,3,3′,4,5,5′-hexaCB	0.39 ± 0.04	0.17 ± 0.02	0.09 ± 0.03	0.09 ± 0.02	0.10 ± 0.03
5′-$MeSO_2$-CB156	ND	0.004 ± 0.001	ND	ND	<0.001
6′-$MeSO_2$-CB156	ND	ND	ND	ND	<0.001

[a] Values represent mean ± SE for three or four rats. [b] ND means not detected.

Table #4 below gives a summary of the distribution ratio of hydroxy and methylsulfonyl metabolites in the liver and the blood of the Wister rats used in this study. The ratio of hydroxy metabolites to unchanged CB values are much higher in the blood than in the liver proving a higher retention of metabolites for the blood than the liver. The ratio of hydroxyl to methylsulfonyl metabolites in the liver are highest for CB156 and the lowest value is for CB118 proving that the metabolites are present in higher concentrations in the CB156 treated rats. In the last column the blood and liver ratio of hydroxyl metabolite are higher in the CB105 treated rats and lowest for the CB156 treated rats.

Table 4. Distribution Ratio of Hydroxy and $MeSO_2$ Metabolites between Blood and Liver

PCB congener	ratio of hydroxy: unchanged CB		ratio of hydroxy:$MeSO_2$ metabolites in liver	blood:liver distribution ratio of hydroxy metabolite
	blood	liver		
CB77[a]	35.1	0.29	0.9	1.7
CB105	11.2	0.07	28	3.5
CB118	7.4	0.05	6.7	3.0
CB156	0.7	0.01	43	2.3

[a] Data are based on ref *24*.

Figure # 5 below presents a schematic view of hydroxylation of CB105 and CB118 in the rats studied. The first step in these reactions involves the formation of the (4, 5) epoxide, then oxygen insertion in pathway B, followed by a removal of a chlorine atom in pathway C with an NIH shift of the 4^{th} carbons chlorine substituent in pathway D.

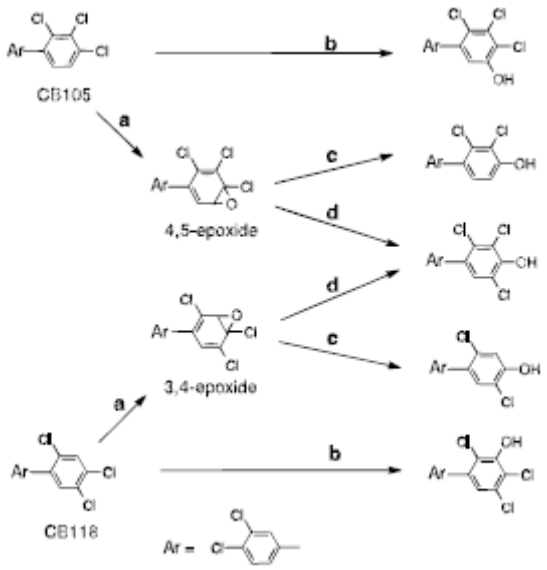

The purpose of this study was to determine the retention of toxic PCB's in the blood and tissues of the animals tested in this article. The metabolism of pentaCB and hexaCB substituted congeners show a lower formation of methylsulfonyl metabolites than the hydroxyl products. In this study the blood of the rats retained the highest percentage of hydroxyl metabolites oppose to the other organs and tissues tested. The hydroxyl metabolites retained were formed due to a NIH shift at the 4th position chlorine substituent. In the future scientist can use a different species of animal along with other PCB's to survey the retention of these toxic chemicals in animals and humans to further examine the role of these metabolites.

Article #3

Title: Influence of Steric Bulk and Electrostatics on the Hydroxylation Regiospecificity of Tryptophan Hydroxylase: Characterization of Methyltryptophans and Azatryptophans as Substrates

Summary:

Tryptophan hydroxylase is one of three pterin-dependent enzymes that catalyze the hydroxylation of certain amino acids. There is little information available about tryptophan hydroxylases mechanism due to the scarceness of its resources and its instability. There were improvements in the development of a stable form of this enzyme that were used in this study. Previous studies suggest that it is the rate limiting step in the reaction that involves the formation of serotonin. The authors in this article use a number of methyl tryptophan substituents and azatryptophans to better understand the hydroxylation mechanisms involving this enzyme. The hydroxylation regioselectivity and the substrate specificity of this enzyme are examined and the results are reported. There was a truncated form of rabbit tryptophan hydroxylase that is prepared using the Moran method. The 6-methyltetrahydropterin used in this study was bought from B. Schircks laboratory. The L-tryptophan, L-5-hydroxytryptophan, DL-4-methyltryptophan, DL-5-methyltryptophan, DL-6-methyltryptophan, DL-7-methyltryptophan, and DL-7-azatryptophan were all obtained from Sigma chemical company and synthesis using the methods from Sloan and Phillips were utilized for L-4-azatryptophan, L-5-azatryptophan, and L-6-azatryptophan. L-2-azaisotryptophan was made using the method described by Tanaka. The D-amino acid oxidase was purified using the method of Fitzpatrick and Massey, and the L-amino acid oxidase and dihydropterin reductase were bought from Sigma chemical company. The tryptophan 2-monooxygenase was made using the method of Emanuele and the catalase was bought from Boehringer Mannheim. The D-amino acid oxidase was used to determine the extinction coefficients of the DL methyltryptophans and the DL azatryptophans. The extinction coefficients of the L-azatryptophans were determined in phosphate buffer. In this experiment the kinetic parameters were found

using four enzymatic assays and the amino acid products in this study were separated and purified using HPLC. The four assays include a continuous fluorescence assay used to find the rate of formation of tryptophan and 7-azatryptophan, a discontinuous HPLC flouresence assay used for the methylated tryptophans, a coupling assay used for 2-azaisotryptophan and 4 &6-azatryptophan utilizes an assay that monitors the changes in the spectrum after hydroxylation of the amino acid. Electrospray mass spectra and NMR analysis where used to identify the structures of each amino acid. The azatryptophans used in this study are isosteric with tryptophan and the methylated tryptophans are used to examine their steric interactions.

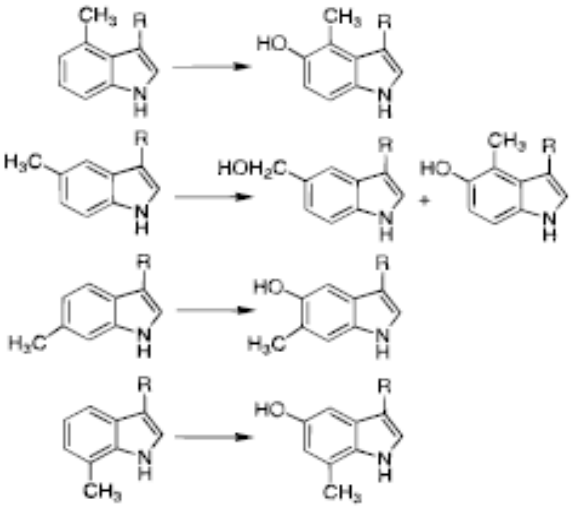

FIGURE 1: The products of hydroxylation of methyltryptophans by tryptophan hydroxylase. In each structure R═CH_2CHNH_3COO.

The products of the hydroxylated methyltryptophans are shown in figure #1. The methylated tryptophans used were hydroxylated by the enzyme, and the resulting product is 5-hydroxy amino acid. The hydroxylation occurs on the 5th carbon of the methylated ring showing a preference for that position in the hydroxylation of these enzymes

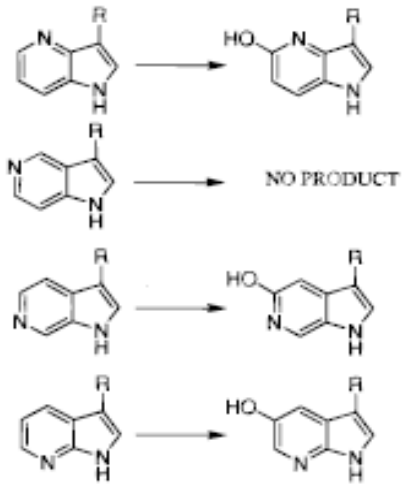

FIGURE 2: The products of hydroxylation of azatryptophans by tryptophan hydroxylase. In each structure R═CH_2CHNH_3COO.

Figure #2 shows the amino acid products formed when azatryptophan is used as the substrate for the enzyme. There are three hydroxylated amino acids that result and they are identified as 4-, 6-, and 7-azatryptophan. When the nitrogen is at the 5th position of the structure there is no resulting product as seen in the 2nd reaction above. The scheme proves that the hydroxylation occurs on the 5th position of the three products observed in the scheme above. Showing a preference for the 5th carbon on the ring when azatryptophan is the substrate and when the nitrogen isn't on the 5th position.

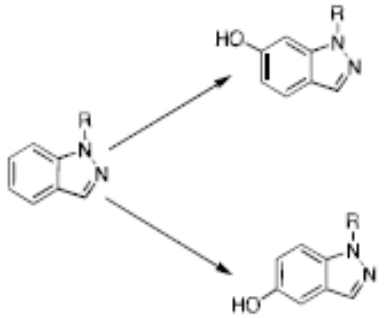

FIGURE 3: The products of hydroxylation of 2-azaisotryptophan by tryptophan hydroxylase. R═CH_2CHNH_3COO.

In figure #3 above the hydroxylation of 2-azaisotryptophan gives two products that are identified as 5-hydroxy-2-azaisotryptophan and 6-hydroxy-2-azaisotryptophan. The hydroxylations move to the sixth position on the ring with 2-azaisotryptophan.

Table 3: Apparent Kinetic Parameters for Tryptophan Analogues as Substrates for Tryptophan Hydroxylase[a]

amino acid	K_m (μM)	$V_{\text{amino acid}}$[b] (min^{-1})	$V/K_{\text{amino acid}}$[b] (mM^{-1} min^{-1})	V_{Pterin}[c] (min^{-1})	amino acid hydroxylated/ tetrahydropterin consumed[d]
tryptophan[e]	2.1 ± 0.1	12.4 ± 0.1	5800 ± 200	12.4 ± 0.1	1.10 ± 0.06
4-methyltryptophan[f]	994 ± 192	16.4 ± 2.1	16.4 ± 1.1	53.8 ± 6.9	0.30 ± 0.007
5-methyltryptophan[f]	> 16000	nd[g]	0.479 ± 0.005	nd	0.15 ± 0.015
6-methyltryptophan[f]	15.1 ± 0.4	4.4 ± 0.1	210 ± 20	9.2 ± 0.1	0.48 ± 0.03
7-methyltryptophan[f]	37.5 ± 0.3	18.9 ± 1.0	500 ± 70	24.9 ± 1.3	0.758 ± 0.02
4-azatryptophan[h]	262 ± 13	21.5 ± 0.7	82 ± 2	57.1 ± 1.7	0.38 ± 0.03
6-azatryptophan[h]	295 ± 12	32 ± 0.7	93 ± 2	77.6 ± 1.7	0.35 ± 0.01
7-azatryptophan[e]	66.2 ± 7.1	15.1 ± 0.9	230 ± 10	15.1 ± 0.9	1.15 ± 0.14
2-isoazatryptophan[i]	86.5 ± 33	13.0 ± 2.0[i]	150 ± 30[i]	19.8 ± 3.0	0.66 ± 0.069

Table #3 above summarizes the kinetic parameters for the eight tryptophan substrates examined for this enzyme. From these values given it was determined that seven of the eight compounds, has an excess of tetrahydropterin consumed. The V/K values given for the 4 & 5 methyl tryptophans are (16.4+/-1.1) & (0.479+/-0.005) respectively. These values are lower than the 6 & 7 methyl tryptophans whose V/K values are (210+/-20) & (500+/-70), respectively. When the azatryptophans are used V/K values were smaller than the 6 & 7 methylated V/K values. The smallest V/K value is the 4-azatryptophan (82+/-2), the 6-azatryptophan value is (93+/-2), and the 2-isoazatryptophans value is (150+/-30), and the 7-azatryptophan has the largest V/K value of (230+/-10). The azatryptophans show larger Vmax values than tryptophan.

Table 4: Mulliken Atomic Charges for Tryptophan Analogues[a]

amino acid	C4	C5	C6	C7	CH_3
tryptophan	−0.20	−0.23*[b]	−0.21	−0.22	
4-methyltryptophan	0.06	−0.26*	−0.20	−0.23	−0.50
5-methyltryptophan	−0.24	0.02*	−0.23	−0.21	−0.50*
6-methyltryptophan	−0.19	−0.25*	0.04	−0.26	−0.51
7-methyltryptophan	−0.21	−0.21*	−0.25	0.05	−0.59
4-azatryptophan	−0.58	−0.04*	−0.28	−0.16	
5-azatryptophan	0.08	−0.55	−0.06	−0.28	
6-azatryptophan	−0.26	−0.04*	−0.54	0.06	
7-azatryptophan	0.14	−0.29*	0.06	−0.60	
2-isoazatryptophan	−0.21	−0.23*	−0.23*	−0.18	

	C2	C3	C4	C5
phenylalanine	−0.23	−0.19	−0.21*	−0.19
tyrosine[c]	−0.20	−0.26*	0.40	−0.26*

Table # 4 list the atomic charges of the indole rings of the different tryptophan analogues

used. Eight of the series of nine methylated and azatryptophan substrates used to investigate the hydroxylation regioselectivity of the enzyme tryptophan hydroxylase are substrates for the enzyme. From the values given in table # 3 it was determined that seven of the eight compounds, has an excess of tetrahydropterin consumed. The 5-azatryptophans were not a substrate for the enzyme and the 2-isoazatryptophan is the only amino acid without a nitrogen atom on the 1st position of the ring, which is important in the positioning of hydroxylation. There is a NIH shift of a methyl group from carbon 5 to carbon 4 that in turn forms the product 4-methyl-5-hydroxytryptophan. The hydroxylating intermediate is very regiospecific and does not hydroxylate at C4 or C6, but this intermediate can oxygenate the benzylic carbon. The study shows that this enzyme is most reactive when the substituents are at the 4th and 5th position of the indole ring. Future studies can determine if different tryptophan analogs can be used to provide better understanding of the tryptophan hydroxylase mechanism and help to provide insight into this enzyme now that there is a stable form available for use.

Article #4

Title: On the Catalytic Mechanism of Tryptophan Hydroxylase

Summary:

Tryptophan hydroxylase is an enzyme that's used as the catalyst in the hydroxylation of amino acids. The purpose of this study is to gain insight into tryptophan hydroxylase catalytic mechanism. There is not a lot of information regarding the catalytic mechanism of this class of enzymes because of the scarceness of resources associated with them. The authors provide some insight regarding this enzyme's mechanism by using a recent

developed stable version of this enzyme to probe its catalyst activity. Previous studies show that this enzyme produces 5-hydroxytryptophan by the hydroxylation of tryptophan and is the rate-limiting step in the catalysis of serotonin. The three pterin-dependent enzymes all require that an NIH shift occur during addition of oxygen when hydroxylating the amino acid. The many materials used in this study were obtained from several laboratories, while synthesis of the compounds utilized different methods. The 6-methyltetrahydropterin (6MPH4) and tetrahydrobiopterin were bought from the B. Schircks laboratory. The tryptophan and 5-hydroxytryptophan were obtained from Sigma Chemical Company and 2H5-Indoletryptophan was from Cambridge Isotope laboratory. The Bosin method was used in the syntheses of 4-2H- and 5-2H-indole and purification of the two indoles was done using HPLC. The deuterated indoles were used in the synthesis of L-4-2H- and L-5-2H-tryptophan using the method of Phillips. The amino acids were purified and the quinonoid dihydrobiopterin was made prior to use. The catalytic core of rabbit tryptophan hydroxylase was prepared using the method of Moran. The methods employed in this article include NMR spectroscopy, HPLC, & fluorescence spectroscopy. The results are reported in terms of the characterization of pterin products using the tyrosine substrate, the deuterium kinetic isotope effects, the NIH shift and the rate of release of the product.

Scheme 1

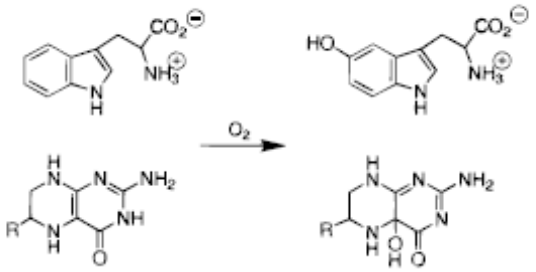

In scheme # 1 shows the hydroxylation of tryptophan to form 5-hydroxytryptophan using the catalytic enzyme tryptophan hydroxylase. In this reaction the tetrahydropterin is converted to a hydroxypterin while the hydroxylation of tryptophan is taking place. During catalysis with TRH the production of hydroxypterin provides evidence there is a reaction involving the oxygen and pterin.

Scheme 2

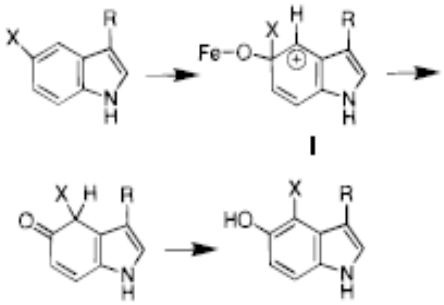

Scheme #2 shows the NIH shift mechanism. In this scheme an electrophilic aromatic hydroxylation with an arenium cation intermediate is shown. Hydroxylation at the 5th carbon on the ring is also seen in this scheme.

Scheme 3

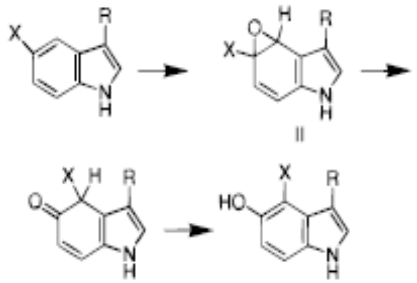

Scheme 3 shows the formation of arene oxide upon oxygen addition by the NIH shift.

In this experiment the authors used a method for characterization of pterin products with tyrosine as substrate.

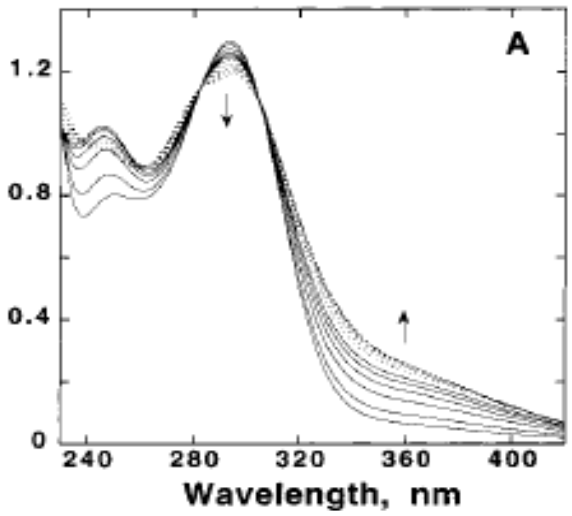

Figure #1a provides the UV/Vis spectral changes showing an increase in the absorbance at 246nm. Hydroxybiopterin absorbance is 246nm and the graph shows there is a 1.0 absorbance at 246 nm, this is in agreement with formation of hydroxybiopterin.

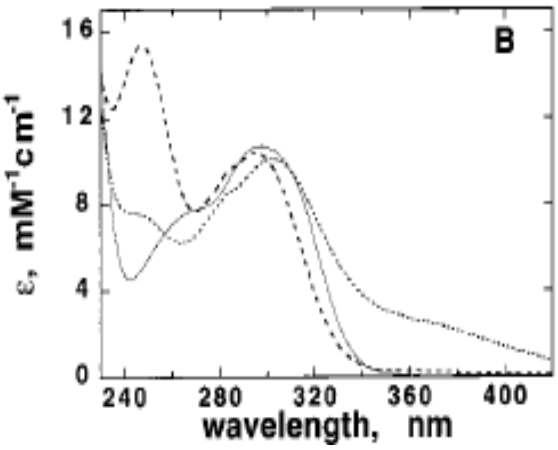

Figure #1b shows the spectra of tetrahydobiopterin, hydroxybiopterin, and quinonoid dihydrobiopterin at 246nm and figure 1c is the comparison of the simulated absorbance traces at 246nm. The data obtained in these three graphs are consistent with other results from previous experiments, suggesting oxygen bond cleavage to form the hydroxypterin and the formation of an intermediate before the hydroxylation of the amino acid.

Table 1. Kinetic Isotope Effects for Hydroxylation of Deuterated Tryptophans by Tryptophan Hydroxylase[a]

amino acid	measured DV[b]	equilibrium isotope effect calcd for formation of I[c]	equilibrium isotope effect calcd for formation of II[c]
$^2H_5$-indole−tryptophan	0.91 (0.88, 0.96)[d]	0.889	0.806
5-^{2}H−tryptophan	0.93 (0.84, 0.97)	0.931	0.876
4-^{2}H−tryptophan	1.03 (0.98, 1.10)	1.003	0.873

Table #1 explains the kinetic equilibrium isotope effects for hydroxylation of deuterated tryptophans by tryptophan hydroxylase, with the conditions set as stated and the structures of these intermediates calculated using Gaussian 94. The equilibrium isotope effect calculations prove the formation of the arene oxide in the second intermediate results in inverse isotope effects with both 4-H-tryptophan and 5-H-tryptophan. These effects increase when the positions are dueterated. If the cation in the first intermediate

was considered we would only see an inverse isotope effect with the deuterated 5-H-tryptophan. . The isotope effect trends, suggest the formation of cationic intermediate in the initial reaction, suggesting oxygen bond cleavage to form the hydroxypterin and the formation of an intermediate before the hydroxylation of the amino acid.

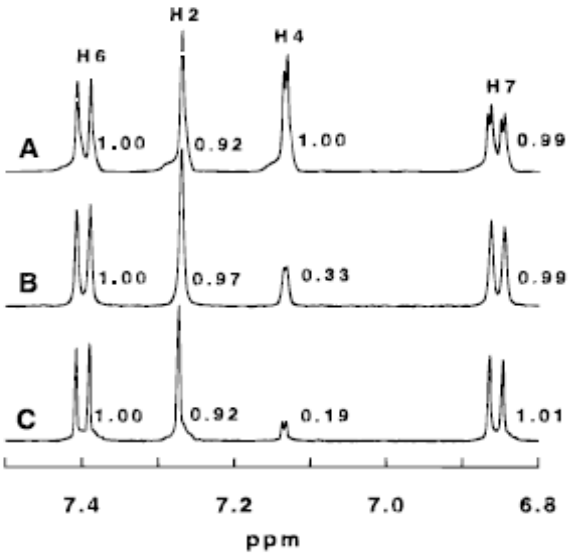

Figure 3. Proton NMR spectra of hydroxytryptophan formed by tryptophan hydroxylase-catalyzed hydroxylation of tryptophan (A), 5-^{2}H-tryptophan (B), or 4-^{2}H-tryptophan (C).

Figure #3 contains three proton NMR spectras of the hydroxytryptophan produced by the catalyzed hydroxylation of tryptophan, with 4-H and 5-H-tryptophan. The formation of 4-H-5-hydroxytryptophan as the product when both 4-H, 5-H-tryptophan are used there is a NIH shift from carbon 5 to carbon 4. In the spectra the amount of the deuterium retained on carbon 4 in the hydroxytryptophan produced were reported as 67% retained at carbon4 when 5-H-tryptophan is the substrate and 81% retained at carbon 4 when 4-H-tryptophan is used as the substrate.

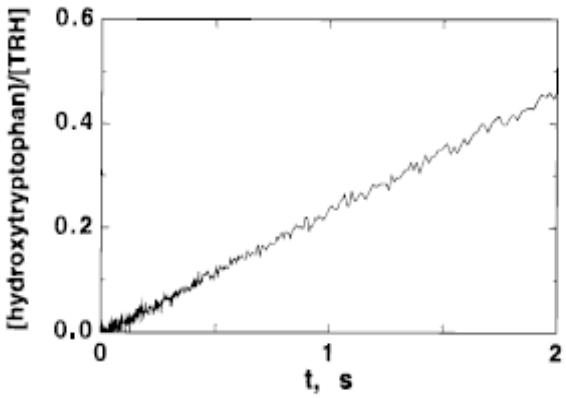

Figure #4 shows a graph of the initial rate of hydroxytryptophan formation showing a fairly linear increase in the formation of the product over time. The graph is used to determine if the amount and rate of hydroxytryptophan formation effects turnover. These results prove the rate of product release does not limit the rate of turnover due to the increase in hydroxytryptophan formation and the linear correlation of the data. The authors in this study employ several techniques for the proposal of a catalytic mechanism of the enzyme tryptophan hydoxylase. The isotope effect trends given in table #1, suggest the formation of cationic intermediate in the initial reaction, suggesting oxygen bond cleavage to form the hydroxypterin and the formation of an intermediate before the hydroxylation of the amino acid. The change in the rate limiting step with this enzyme proves that an increase in the rate of formation of the hydroxylating intermediate, results in a decrease in the rate of turnover. This cationic formation involves the inverse isotope effect when the isotopic exchange happens at the same site the oxygen addition occurs. The formation of 4-H-5-hydroxytryptophan as the product when both 4-H, 5-H-tryptophan are used shows a NIH shift from carbon 5 to carbon 4 The NMR spectral data is consistent with a NIH shift from carbon5 to carbon4 once oxygen attacks the ring of the amino acid substrate and generates a cation. The hydroxylated amino acid product is made once the ring reforms. Scheme # 7 below provides a catalytic mechanism for the

enzyme tryptophan hydroxylase. Future studies can use different amino acid substrates to provide answers to the questions posed about pterin enzymes catalytic mechanism.

Scheme 7

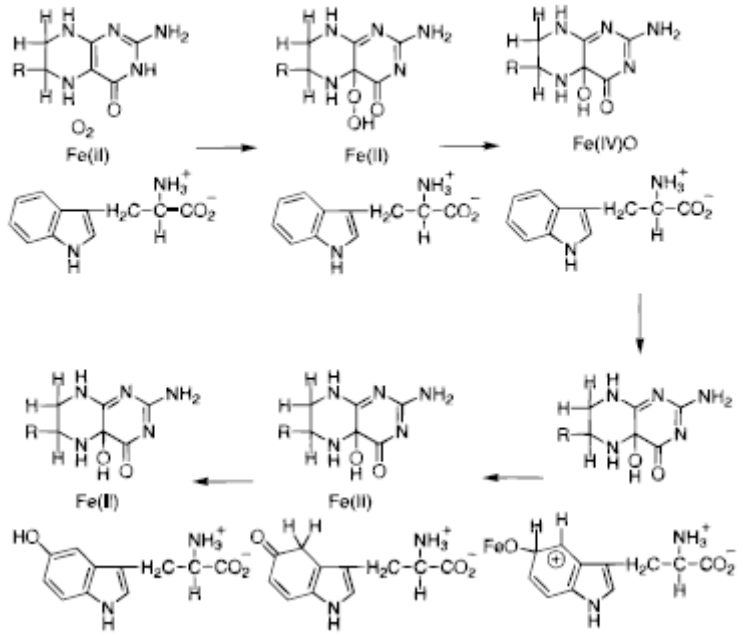

Article # 5

Detection of a “Nonaromatic” NIH Shift during In Vivo Metabolism of the Monoterpene Carvone in Humans

Summary:

In this experiment the authors examine the position of labels found in carvone metabolites during in vivo metabolism of monoterpene carvone in humans. The three monoterpene carvones in this study are responsible for the oxygenating metabolites found in humans. This paper was published in the year 2002, to this date no other publishing’s exist as to the labeling of stable isotopes to probe the oxidation mechanism of the carvone isopropyl group. The authors develop synthetic technique that produces carvone labeled with stable isotopes at a particular site and examine the oxidation mechanism of the

isopropyl group of the monoterpene carvone along with the metabolic pathways of carvone metabolism in humans. The purpose of this study is to determine the position and extent of labeling in carvone which will provide valuable information into the in vivo metabolic pathways of the isopropenyl group. The materials and chemicals used in this study are from numerous laboratories and companies throughout the world. The sodium metaperiodate was bought from a German company named Merck. The triphenylphosphine, D3-iodomethane, 13C-iodomethane, sodium hydride, and butyl lithium were purchased from Aldrich chemical company also in Germany. The methods include synthesis of compounds utilizing several methods, isolation of metabolites, and purification techniques including HPLC. Human experimentation was performed in a prior experiment and the urine collected and tested using MICA experimental procedures. Derivatization procedures and techniques used for isolation of the metabolites from the urine were performed. High-pressure liquid chromatography was used in the purification of the acidic metabolites. Synthesis of 9, 9-Dideutero-Carvone and 9-13C-Carvone via the epoxygenation of carvone with subsequent cleavage of the epoxide by sulfuric acid was performed. NMR spectra were obtained using a Bruker Am 360 instrument and high resolution gas chromatography and mass spectrum were employed also. The results are reported in terms of the mechanisms of oxidative in vivo metabolism, the synthesis of 9,9-dideutero-carvone or 9-13C-carvone, the deuterium distribution in (M1), (M2), and (M3) from 9-dideutero-carvone, the 13C distribution in (M1), (M2) and (M3) from 9-13C-carvone, and mass spectrometric fragmentation of M1-ET and M2-ET, 13C distribution in M2 from 9-13C-carvone.

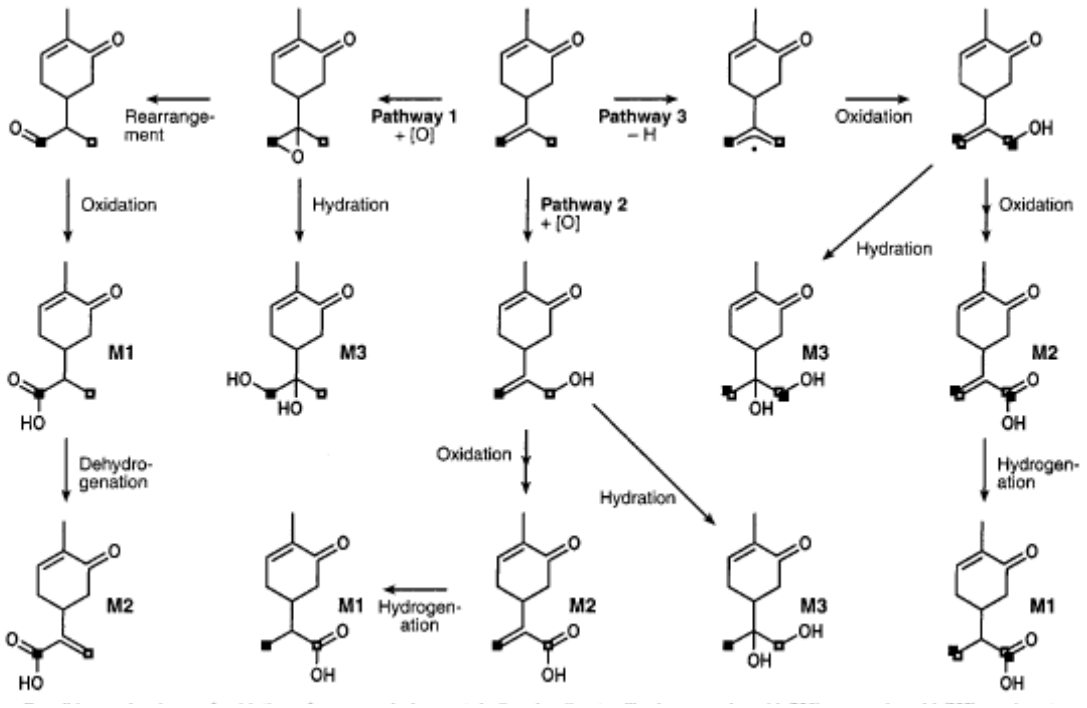

Figure #1 above provides several possible mechanisms of oxidation of carvone during metabolism to dihydrocarvonic acid, carvonic acid, and uroterpenolone. Pathway #1 results in the formation of (M1) or dihydrocarvonic acid. This reaction starts with the addition of oxygen to produce an epoxide as the first intermediate, the mechanism proceeds with an isomerization rearrangement of the oxygen to form an aldehyde, followed by oxidation producing dihydrocarvonic acid (M1). Pathway 2 provides an explanation for the formation of carvonic acid that begins with the hydroxylation of the methyl moiety on the isopropenyl group. This hydroxylation produces an alcohol that can be further oxidized to produce carvonic acid. Carvonic acid in the 2nd pathway can be further hydrogenated to form dihydrocarvonic acid (M1). Uroterpenolone can use either pathway 1, 2, or 3 for formation. Pathway 3 presents a symmetrical radical mechanism as depicted in the scheme.

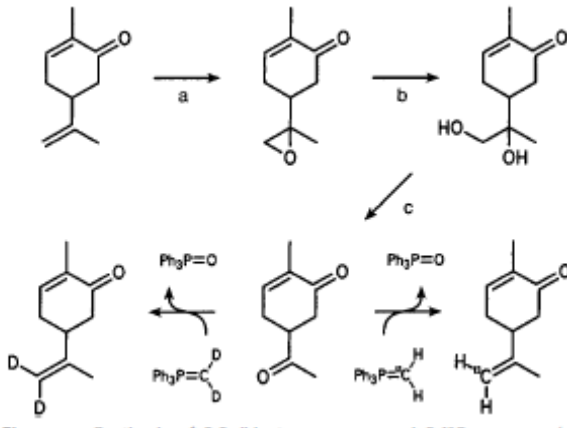

Figure #2 explains the synthesis of 9-9-dideutero-carvone or 9-13C-carvone. This scheme begins with the formation of an epoxide pathway (a) a result of oxygen addition to the unlabeled carvone which forms 8, 9-epoxy-carvone. Hydrolysis of the 8, 9-epoxy-carvone can give uroterpenolone. If there was a cleavage of uroterpenolone this would produces 5-acetyl-2-methyl-2-cyclohexen-1-one which can react to form the deuterated carvone or the 13C carvone. The deuterium distributed among M1 and M2 from the synthesized 9, 9-dideutero-carvone was metabolized and the results were obtained and reported. HPLC was used to purify the extract containing the metabolites after derivatization of the extract with iodoethane. The results of the retention of deuterium in both acids suggest that more than one oxidation method is present in this mechanism. This is evident because of the three pathways there isn't just one, the distribution of deuterium utilizes all three pathways.

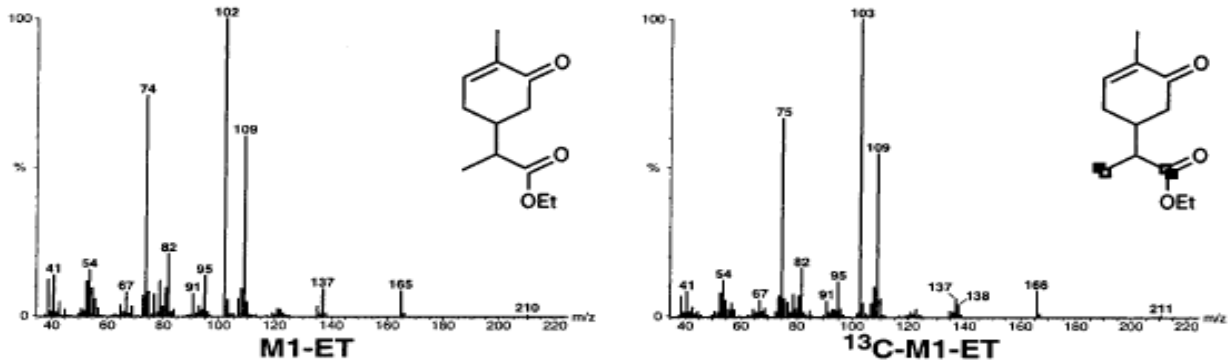

Figure #3 contains the mass spectra of M1-ET and 13C-M1-ET and there proposed fragmentation pattern. The mass spectrum above helps to determine the 13C distribution between the carboxy and the methyl groups. The results suggest that this ion is stable at 137 m/z and is the ion used to the determination of the labeling distribution between the groups. This ion results from a charge induced cleavage of the 165 m/z ion which causes the loss of carbon monoxide to form the 137m/z ion.

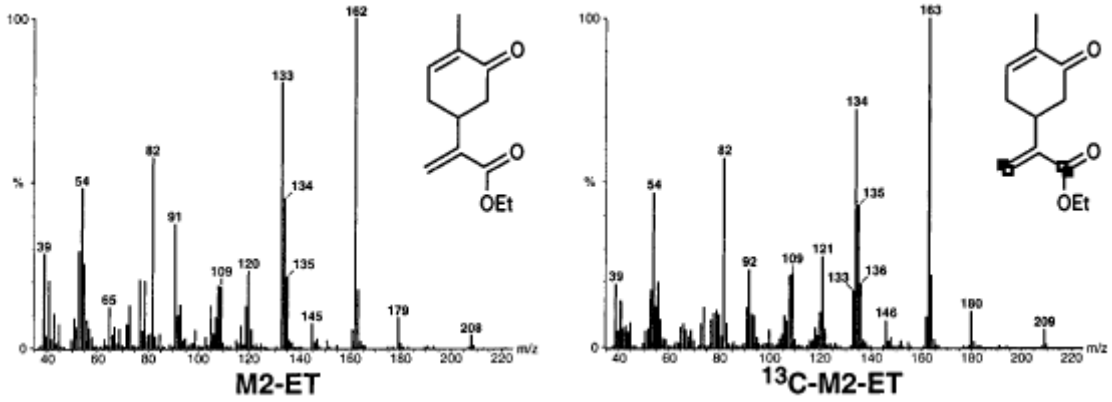

Figure # 4 contains the mass spectra of unlabeled M2-ET and 13C-M2-ET along with proposed fragmentation patterns. The double bonds in M2 allows for a higher intensity than the M1 mass spectra. The ion at m/z 133 appears to be very stable with a higher intensity in the first mass spectrum than in the second one with 13C-M2-ET. This ion is the smallest in the H cluster and is determined to be the ion used for the distribution determination of 13C because of its stability. From the results of the 13C distribution for M1 and M2, the authors conclude that both acids are made by independent pathways due to there opposite distributions. The NIH shift usually involving the hydroxylation of aromatic compounds was detected in this article to occur in a nonaromatic compound. This paper is the first that I've seen to report a nonaromatic NIH shift, when M1 undergoes a hydride shift during oxidation owing to a nonaromatic NIH shift. The

product of this nonaromatic NIH shift is 8, 9-dihydro-carvonaldehyde. When enolization occurs, this will result in lose of some of the hydride in 8, 9-dihydro-carvonaldehyde before oxidation of the compound.

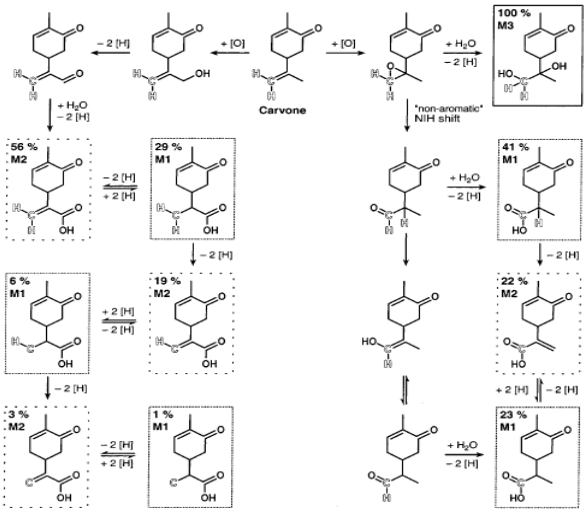

Figure #6 reveals that the 23% of labeled M1 does not contain any of the initial hydrogens from carvone. In this schematic view of the formation of M1, M2, and M3 during in vivo metabolism of carvone in humans, the view provides a trace of the pathways that lead to the major oxygenated in vivo metabolites of carvone in humans. In conclusion the authors provide evidence that the partial transformation of carvone to a carvone epoxide that rearranges to give M1 is apparent. M2 is formed by the oxidation of 10-hydroxy-carvone and M3 can be produced from the carvone epoxide. There was a non aromatic NIH shift that occurs and is the first reported as of this study. In future studies the authors can examine metabolic pathways using different metabolites to gain insight into the mechanism involving the non aromatic NIH shift, this could clarify some of the questions regarding this mechanism that is involved in hydroxylation reactions.

Article #6

Title: Modeling the Mononuclear, Dinuclear, and Trinuclear Copper(I) Reaction Centers of Copper Proteins Using Pyridylalkylamine Ligands Connected to 1,3,5-Triethylbenzene Spacer

Summary:

Biomimetic chemistry allows scientist to mimic the laws of nature by creating synthetic compounds that can be used in place of the natural, less obtainable compounds. In this study the authors used pyridylalkylamine ligands connected to 1, 3, 5-triethylbenzene spacers to represent the mono, di, and trinuclear copper (I) reaction centers of copper proteins. These reaction sites have a wide variety of important functions and are not in abundance in nature, hence, less attainable. 1, 3, 5-triethylbenzene spacers are important in science, they are used for developing receptors, and are important in the steric configuration of functional groups. The triethylbenzene spacer is usually a flexible part of a molecule that provides a connection between two molecules. In this study biomimetic copper chemistry is used to copy the copper (1) reaction sites of copper proteins using pyridylalkylamine connected to 1, 2, 3, triethylbenzene spacer ligands. The chemicals used in this study were all of high purity and of commercial grade, and were obtained from different laboratories and companies. The synthesis of 1,3,5-triethyl-2,4-bis((*N*-benzyl-*N*-(2-(pyridin-2-yl)-ethyl))-aminomethyl) benzene (Pye2), and 1,3,5-triethyl-2,4,6-tris((*N*-benzyl-*N*-(2-(pyridin-2-yl)ethyl))-aminomethyl) benzene (Pye3) was done by adding a mixture of N-benzyl-N-(2(-pyridine-2-yl)ethyl)amine and potasium carbonate in a dry methylcyanide solution, this solution was added to 1,3 -bis and 1,3-tris(bromomethyl)-2,4,6-triethyl and the mixture was stirred. The percipitates were then washed with a methylchloride solution. The yellow residue from the evaporated organic

products were further separated by column chromatography and the resulting product were the (Pye 2) and (Pye3) ligands. The1,3,5-triethyl-2,4-bis((*N*-benzyl-*N*-(6-methylpyridin-2-ylmethyl))-aminomethyl) benzene (MePym2) was prepared by adding N-benzyl-N-(6(methylpyridin-2-ylmethyl)amine intoa mixture of potasium carbonate in a dry methylcyanide solution, this solution was then added to 1,3 -bis and 1,3-tris(bromomethyl)-2,4,6-triethyl and the mixture was stirred. The percipitates were then washed with a methylchloride solution. The yellow residue from the evaporated organic products were further separated by column chromatography and the resulting products were(MePym2) and (MePym3). The [CuI(Pye2)(CF3SO3)and [CuI(Pye3)](CF3SO3) were made by dissolving the Pye2 in acetone and the Pye3 in methanol, into an acetone and methanol solution of [CuI](CF3SO3)and [CuI](CF3SO3). These two solutions were then stirred and the percipitates collected. After recrystallization of the material from an acetone/hexane mixture x-ray crystallography was performed on the powder.The last two compounds, [CuI 2(MePym2)(Cl)]CuCl2, [CuI3(MePym3)(CF3SO3)(CH3CN)3](CF3SO3)2 were made in the manner of which the Pye2 and Pye3 compounds were made.The analytical methods used in this article include FT-IR, UV-Vis spectroscopy, H NMR spectroscopy, Mass spectroscopy, ESI-MS, Elemental analyzer, and Electrochemical analysis. The results in this experiment are obtained and reported in terms of the ligand synthesis of the two mono, bi, and trinuclear Copper(I) complexes, their oxygen reactivity, and the biological relevance of the two mononuclear complexes. The synthesis of the Pye2 and MePym2 ligands employed the Sn2 reaction as seen in the scheme #1 below, using a potassium carbonate and acetonitrile solution. The Pye3 and MePym3 were made in the same manner but using

different chemicals, and is dipicted in scheme #1 that follows.

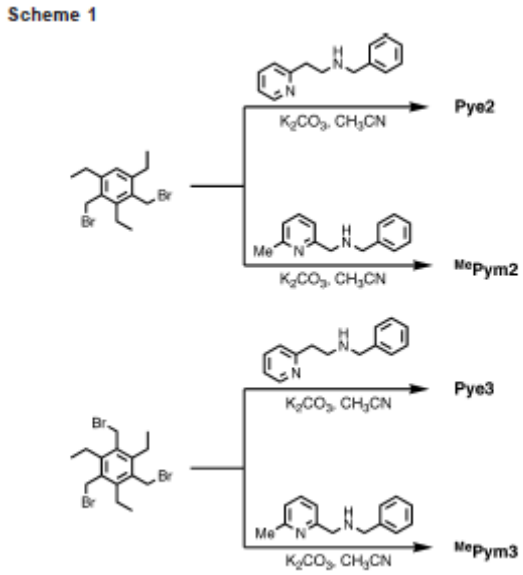

Scheme #1 provides an explanation of the bis and tris (didentate) ligand synthesis. Pye2 and mePym2 were made by using a bis spacer and Pye3 and Pym3 were synthesized using a tris triethylbenzene spacer, further treatment with a copper (I) complex gives the resultant four copper complexes. Pye2 has two metal binding sites and a two-coordinate linear shape, while the Pye3 ligand has three metal binding sites that have a copper (I) center with a three-coordinate trigonal planar shape. Complexes 1 and 2 both have no reactivity towards oxygen, due to there high oxidation potentials. The shape and structure of Pye3 is very close to the CuA site of the PHM monooxygenase.The ion at the CuB site in cytochrome c oxidase has a t-shape that is close to the Pye2 geometry. MePym afforded the dinuclear copper (I) complex, the chlorine atom bridges the two copper ions at a ~93.3 degree angle, and a distance between the copper ions of ~3.186 angstroms. This gives the structure a trigonal planar shape but due to its short bong length between copper ions, is not a good system for the copper proteins. This compound shows reativity towards dioxygen, which makes this a good mimic for the enzyme tyrosinase. The

trinuclear copper (I) complexes shape exhibits a C3 symmetry and the three copper ions have the trigonal pyrimidal shape. The trigonal shape is similar to ascorbate oxidases reaction centers and the compound also affords some reactivity towards dioxygen. There are two hydroxylated compounds that result from complex 3 and complex 4 which is proof of there reactivity with dioxygen. Complexes 5 and 6 and there mechanism is provided in scheme 2 below. These two complexes exhibit an NIH alkyl shift where the ethyl group of the spacer migrates in a 1, 2 shift and the hydroxylation occurs at the site that the ethyl atom leaves. The NIH shift in these rearrangement show evidence of a cationic intermediate but there was not an intermediate found in this study.

Scheme 2

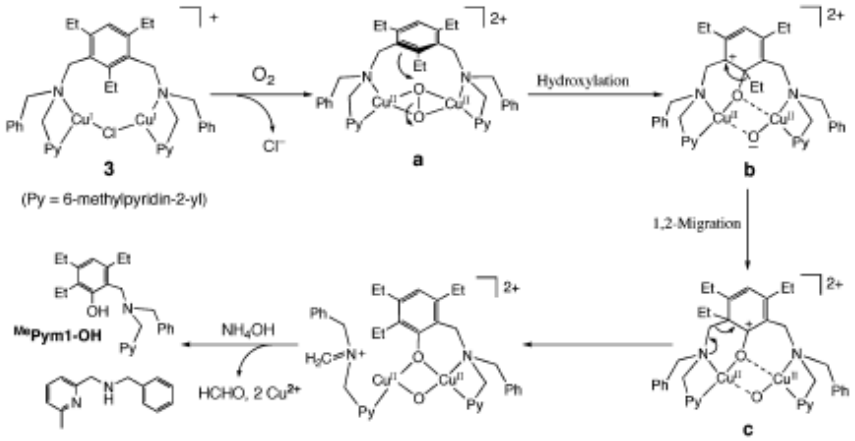

In conclusion this article uses biomimetic synthesis using the pyridylalkylamine ligands connected to 1, 3, 5 triethylbenzene spacers to mimic the mononuclear, dinuclear, and trinuclear copper (I) complexes used as active sites for copper proteins. The oxygen reactivity of these centers is examined too. The dinuclear and trinuclear copper (I) complexes 3 and 4 both react with oxygen unlike the mononuclear copper (I) complexes which have very high oxidation potentials and thus little or no reactivity with oxygen. Complex 5 and 6 are mononuclear and dinuclear copper (II) complexes that results from

the hydroxylation of the aromatic ring structure. In the dimeric copper (II) complex, the NIH shift of the ethyl group is seen and the hydroxylation reaction provides evidence of the formation of a cationic intermediate that was not found in this study. Chart #1 gives the structure of the four pyridylalkylamine ligands created in this article, which include complex 1 (PYE2), complex 2 (PYE3), complex 3 (MePYM2) and complex 4 (MePYM3). In the future the synthesis of these compounds to mimic less attainable compounds should continue in order to probe the mechanisms of the Copper(I) reaction sites.

Article #7

Title: Biomimetic Aryl Hydroxylation Derived from Alkyl Hydroperoxide at a Nonheme Iron Center. Evidence for a FeIVdO Oxidant

Summary:

Biomimetic chemistry involves the study of human-made processes, substances, devices, or systems that imitate nature. Previously, a NIH aryl shift with oxygen atom transfer has been observed giving proof of an intermediate in these reactions. In this study the synthesis of an iron (II) complex is used to investigate the mechanism of aryl hydroxylation reactions using non heme iron centered enzymes to provide insight into there mechanism and kinetics in these reactions. The methods used are proton NMR spectroscopy, UV-visible spectroscopy, Electrochemical analysis and mass spectrometry FT-IR. The majority of the chemicals used in this study were obtained from the Aldrich chemical company. These chemicals were ACS grade and the bulk solvents were dried

and degrassed using routine methods. The aryl boronic acid was obtained from two companies, Aldrich and Lancaster chemical companies and the solvents used in NMR were purchased from the Cambridge Isotope Labs. The Pd (PPh3) compound was from the Lancaster chemical companyand the bis-(2-Pyridylmethyl) amine was bought from the Richman chemical company. The synthesis of (MPPH), bis-amine, 6-bromo-2-pyridinecarboxaldehyde the iron (OTf)2 and the ortho-d1-bromobenzene were employed by utilizing procedures from previous synthesis methods. The results are described using the synthesis and proton NMR of the ligands and iron (II) complexes, the reaction with BuOOH, spectroscopy to detect the reaction intermediate and other mechanistic probes.

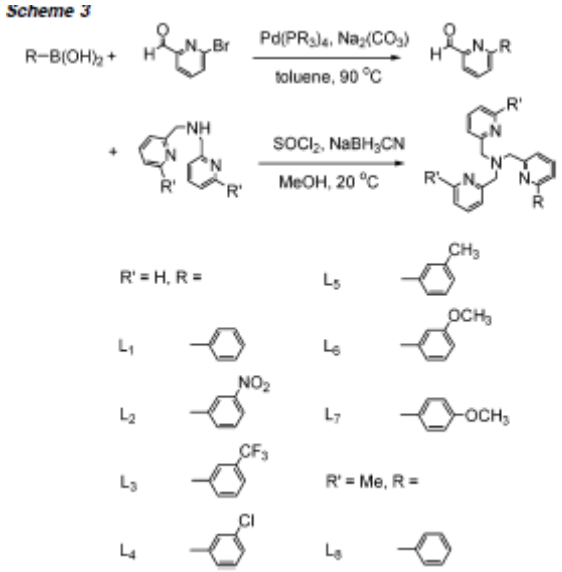

Scheme 3 aboves shows the resultant ligands and their synthesis. The authors add different alpha aryl substituents along with electron withdrawing functional groups at the meta position to form the L2-L6 ligands. These meta substituents help in the manipulation of the electronic properties at the ortho position, while the aryl substituents allow for aromatic electrophilicity of the ring. The NMR data proves this by the desheilding effects of the meta substituents on the para and ortho positions. The para and

ortho proton resonances described provide evidence that supports the notion that the ipso and other meta protons were unaffected by the meta substituents. The iron (II) complexes were made by mixing the Fe (II) (OTf) 2 and 2 methylcyanide together yeilding neutral iron (II) complexes dissolved in methylcyanide to form bis salt cations. There were three complexes obtained namely L1, L6, and L8. L1 and L6 have a geometry that is similar in comparison to the tetradentate ligands, a pseudooctohedral coordination which provides open cis sites and a pyridine with two ligands. The bond lengths are described as being in the range of (~2.18 & ~2.22) which is evidence of a high spin iron (II) state for the L1 and L8 complexes, with the exception of L6 that has a slightly higher bond length making this complex non symmetric. When the seven triflate complexes dissolved in methylchloride were examined, the light yellow solution gave a poor signal with very low absorption in the 350nm-380nm region. In the organonitrile solution the iron (II) and pyridine shows strong absorbance signals at 330(+/-) 5 nm and 400(+/-) 5 nm and a small but broad weak signal at 550 nm in the ligand field. The organonitrile solutions have better absorbance than the methylchloride solutions due to the color change. The results show that the weaker ligand fields are attracted to the iron (II) ion. This provides a practical method that can be used once the stable chromophors are developed. The reaction of the complexes with methylcyanide and the peroxide (BuOOH) provided the experimenters with stable chromophors that can be detected using UV/Visible spectroscopy.

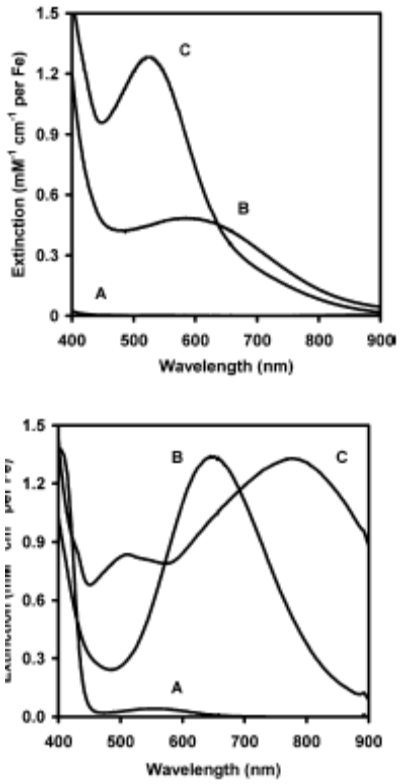

Figure # 4 shows the visible spectra of the L1 and L8 complexes, (A) provides the absorbance of iron(II) methylcyanide, (B) is the iron(III) peroxide intermediate, and (c) is the product with. The L1 graph was recorded at 228K and the L8 graphs temperature is at 293K. The absorbance of (A) in both figures appears to be very weak and broad on the bottom graph, with a shoulder at 550nm the top graphs signal can barely be seen. The signal for the (B) intermediate appears very strong around 650nm on the L1 graph, while the absorbance band on the L8 graph with a higher temperature appears broader but not as intense a peak around the same wavelength. The product (C) has the most intense signal in both graphs, although the absorbances appear at different wavelengths. The L8 complex shows a broad peak at ~ 530nm, while the L1 graph has a broader signal for (C) at 780nm due to the displacement of the methylchloride with oxide ligands. The L2, L3, and L4 complexes containing aryl substituents caused a blue shift, while the L5 complex

was red shifted relative to the L1 chromophor. This red shift is due to a decrease in the basicity because of the methylated ligand. These chromophores in these complexes show evidence of an otho hydroxylation of the pendant arenes with LMCT bands that are characteristic of the phenolate to iron (III) bands. There was an oxo-dimer detected in the L1 complex that was further examined using X-ray crystallography.

In figure 7 the oxo-bridge shows a rigid symmetrical structure that usually forms during hydroxylation. Scheme 6 and scheme 7 depicted below shows free radical initiation and electrophilic substitution by metal centered oxidants.

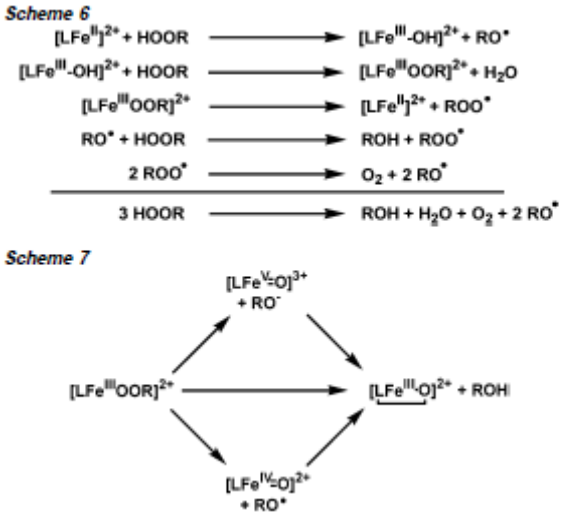

The resultant data proves that the spin state was retained for iron (II) in solution. The products of L1-L8 oxidation are [(L1O-) FeIII(X)] 2+ and [(L8O-) 2 FeIII 2(O)] 2+, and the product distribution proves that a benzyl radical forms from the hydroxylation mechanism. This study proves that arene hydroxylation in iron (II) complexes involves an one-electron oxidation of the iron complex by the peroxide to an iron (III) alkylperoxo

intermediate. To break down the peroxo intermediate, the arene hydroxylation must be coupled. Efficient hydroxylation of arenes are observed when the iron (III) complexes with peroxide or dioxygen/ascorbic acid are used. The results provide evidence of an oxoiron(IV) in the arene hydroxylation reactions that result in an NIH shift.

Article #8

Title: 14C- and 3H-Tyrosine Incorporation into Ascidia Ceratodes Tunichrome in Vivo

Summary:

In this study the authors examine radio labeled tyrosine as a possible reason for the production of tunichrome in the morula cells of blood. The authors use 14C and 3H-tyrosine to determine the specificity and distribution of the labeled compounds to better understand incorporation of tyrosine into tunichrome. Earlier studies conducted experiments that incorporated radiolabled phenylalanine into tunichrome, but were not sure if the catechol and pyrogallol moieties were formed prior to or after the tunichrome backbone forms. Hydroxylation of the benezene ring could happen before the formation of the tunichrome backbone if tyrosine, with its hydroxyl moeity, is incorporated as easily as phenylalanine is incorporated into tunichrome. The hydroxylation of the benzene ring before the formation of the tunichrome backbone would prove evident if the radiolabeled tyrosine is easily incorporated into the tunichrome. The purpose of this article is to determine if an already hydroxylated species can be incorporated into tunichrome in vivo. The chemicals and specimen were obtained from several suppliers. The A.ceratodes used in this experiment was kept in an aerated aquaria after being purchased from Sea Life Supply Company. Several of the A. ceratodes were exposed to

tyrosine and sea water for 24-26 hours. The animals were removed from the control area and placed in clean water and tested regularly using the blood removed and centrifuged to separate the blood cells from the plasma. Acetic anhydride and pyridine were used for tunichrome acetylation and separation of tunichrome from other hemocytes using thin layer chromatography. The tunichrome TLC band is removed from the plate and washed repeatedly with isopropanol in methylchloride and evaporated under a steam of nitrogen. The tunicate acetate residue is dissolved in methyl cyanide and a sub-sample is stored and its structure is confirmed using HPLC. A scintillation vial is used for drying of the remaining samples in peroxide and exposure to 1 of 2 scintillation cocktails overnight for equilibration. The tunichrome on the TLC plate was identified utilizing reverse phase HPLC, and the remaining bands were also examined for there radioactivity and analyzed using HPLC. The blood and plasma of the A. ceratodes were assayed for there radioactivity and homogenization in distilled H2O, using the four pooled bodies from each of the two previously mentioned experiments in distilled H2O. The subsamples that contained a tissue solubilizer, were weighed in scintillation vials and digested for one day. The experimenters added a gold scintillation cocktail and the vials were equilibrated without light overnight and there radioactivity was analyzed. The tunic samples utilized the same methods previously mentioned but were homogenized in tissue solubilizer, while the plasma samples were exposed to peroxide overnight and scintillation cocktail were added. The analytical methods used in this article include TLC, HPLC, and UV/VIS. The rate at which tyrosine was incorporated into tunichrome is comparable to the rate of phenylalanine incorporation in previous studies.

Figure #2 below shows that there is a decline in both tyrosine and phenylalanine

concentrations in seawater over time. The graph reveals that the tyrosine concentration shows a rapid decline over a three to five hour period for the 14C-tyrosine, and only a small decline in a couple of hours for the radio labeled 3H-tyrosine. The phenylalanine and the tyrosine follow the same pattern, after one day the seawater concentration for both reach almost zero. There was a small rise in the 3H-tyrosine as time elapsed but was at it lowest after five hours. The increase may be due to the 3H-tyrosine acting as a metabolite in the animals and being excreted by the organisms thus causing an increase as time elasped.

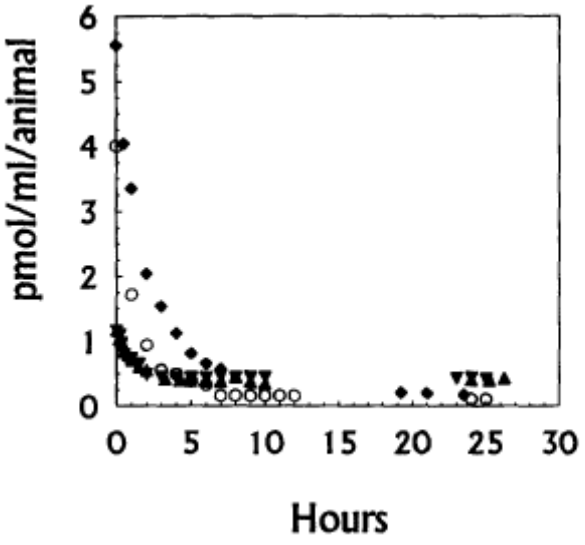

Tyrosine half life is calculated and was 1.6-2.2 hours, which was double that of phenalanine at 1.1 hour, owing to tyrosine being removed at a slower rate. The fluorescing compounds that contained the labeled tyrosine were separated from the TLC plates and analyzed using reverse phase HPLC.

Figure #3 below reveals that the bright orange and the pumkin color bands have Rf values of 0.35 & 0.39 with the concentration of tyrosine at its highest values in pmole at 0.0156 & 0.0374 respectively. After analysis with RP-HPLC the pumkin band was

determined to be the one band that contained the acetylated tunichrome.

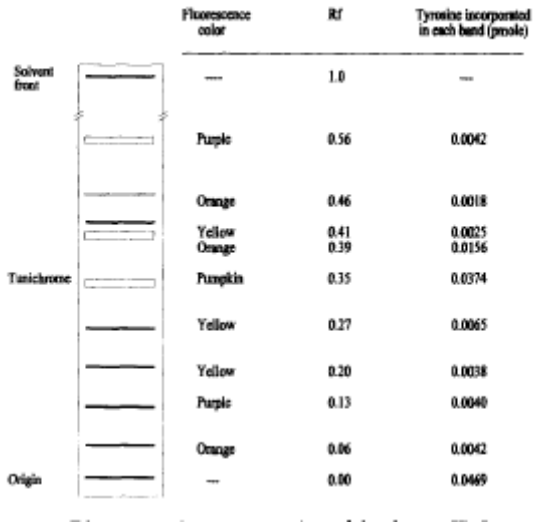

	Fluorescence color	Rf	Tyrosine incorporated in each band (pmole)
Solvent front	---	1.0	---
	Purple	0.56	0.0042
	Orange	0.46	0.0018
	Yellow	0.41	0.0025
	Orange	0.39	0.0156
Tunichrome	Pumpkin	0.35	0.0374
	Yellow	0.27	0.0065
	Yellow	0.20	0.0038
	Purple	0.13	0.0040
	Orange	0.06	0.0042
Origin	---	0.00	0.0469

Figure #4 presents a graph of the concentration of tyrosine and phenaylalanine label tunichrome showing a fairly linear increase overtime in both. It also shows that on days 7, 9, &11 the concentration of tyrosine was high compared to phenylalanine and days 14, 30, & 37. This data proves that tyrosine is incorporated into tunichrome at a rate similar to phenylalanine.

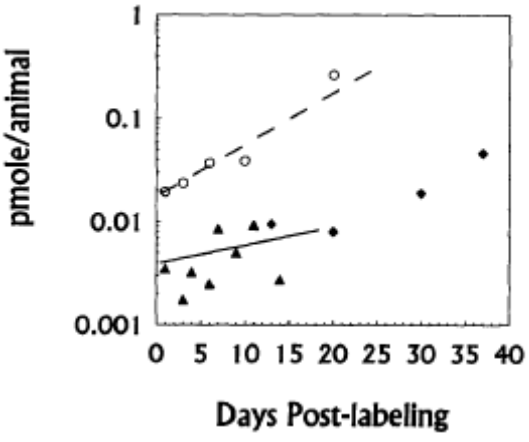

Table #1 provides the amount in pmole/animal of tyrosine label in the other tissues studied. The tunic has the highest values over the entire length of the experiment. While

the whole blood is next with values at 136 on day one and a varied decline for the remainder of days. The blood plasma has the next smallest volume of label, and the tunichrome only has minute to nearly zero concentrations of labeled tyrosine. These results show that the tunic has the highest concentration of radiolabel, then whole blood and blood plasma, but tunichrome had the smallest amount of radiolabel tyrosine incorporation.

TABLE 1. Total amounts of tyrosine (pmol/animal) incorporated into the tunic, whole body, blood plasma and tunichrome TLC band of *Ascidia ceratodes* exposed to 1.2 pmol/ml/animal of ^{3}H-tyrosine (Expts. 2 and 3 combined). Measurements were made on pooled samples of four organisms per sampling time

Day	Tunic	Whole body	Blood plasma	Tunichrome
1	190	136	11.6	0.004
3	121	50	3.6	0.002
4	124	14	1.3	0.003
6	121	60	4.3	0.002
7	144	22	1.2	0.008
9	94	30	2.6	0.005
11	106	19	1.1	0.009
14	80	14	0.6	0.003

In this study the authors provide evidence that tyrosine can be incorporated into tunichrome in vivo with a higher rate constant than phenylalanine and tunichrome synthesis occurs at a lower intracellular concentration of tyrosine than phenylalanine, which is evident by its low y- intercept value. When the 3, 5 L-tyrosine was used the 3 and 5 carbon site were hydroxylated and is a requirement for the biosynthesis of tunichrome. The pyrogallol moiety of tunichrome retains a small percentage of the tritium label and is consistent with the NIH shift mechanism. This loss of tritium proves that tyrosine can be incorporated into tunichrome in vivo. Further studies into and refinement of the labeling technique and better separation methods could provide a better understanding of the mechanisms in the biosynthesis of tunichrome.

Article # 9

Biotransformation of Cubenene to 7-hydroxycalamenene in cultured cells of the liverwort, Heteroscyphus planus

Summary:

Heteroscyphus planus is a leafy plant that possesses a gametophyte and a sporophyte stage in their lifecycle. This plant has a taxonomic genus and it belongs to the Geocalycaceae family. Cubenene is a sesquiterpene that has a naphthalene ring with hydrogenation on several positions of the ring. The sesquiterpenes studied in this article are seen in terrestrial plants and invertebrates and thus is important in nature. The purpose of this study is to examine the biosynthesis of 7-hydoxycalamenene in the heteroscyphus planus cultured cells of liverworts. There is little evidence as to the mode of aromatization or how the hydroxyl group adds to the ring and previous studies suggest that there is no NIH shift when malvonic acid is used in the synthesis of 7-hydroxycalamenene. The authors provide direct evidence of the conversion of cubenene to 7-hydroxycalamenene with hydroxylation of the ring occurring without a NIH shift. The analytical methods used include GC/MS, proton NMR, reverse phase-HPLC, and UV spectroscopy. The (-)-alpha-cubenene used was bought from Fluka Chemie. The sesquiterpenes concentrations were estimated using calibration curves from compounds 2, 10, &11 and detected by UV spectroscopy. The results explain the preparation of the precursors and the biotransformation of cubenene and calamenene. There were several deviations from others methods used in earlier studies in the synthesis of cubebene (10) and calamenene (11) borrowed for the conversion of (-)-alpha-cubebene (7). In figure 2 the chemical conversion of (-)-alpha-cubenene (2) in TFA is shown. The figure shows the

three dienes 8, 9, & 10 that formed from one equimolar amount TFA and (7). The fourth compound (11) was identified using proton NMR, the results show the formation from the ten equimolar excess of TFA with (7).

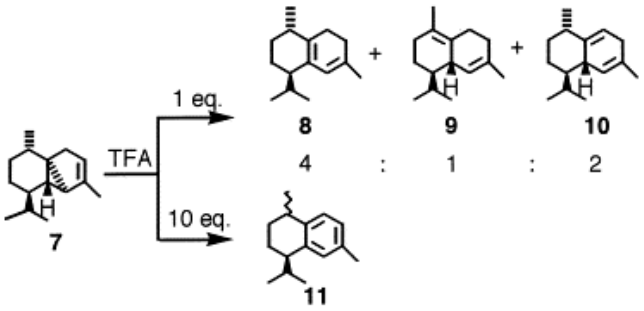

The synthesis of [2H6]-calamenene (13) was carried out utilizing a previous method and [2H7]-4'-methyl acetophenone (12) shown in figure 3. This compound (13) undergoes the birch reduction mechanism and produces the diene (14) rather than the anticipated cubenene (10).

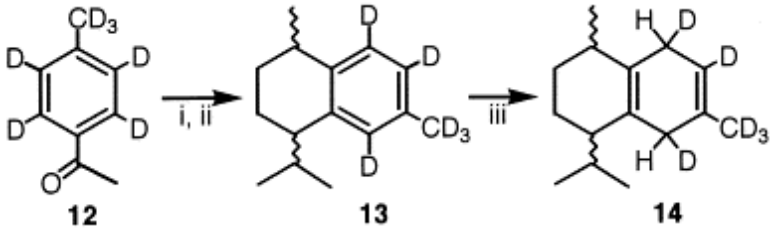

Figure 4 below shows the three compounds used in the synthesis of [2H2]-cubenene (17). Oxidation of compound (15) utilizes pyridinium chlorochromate, compound (16) was prepared using the methods of Cane, and Tandon and upon dehydration of compound (16) the resultant compound (17) forms.

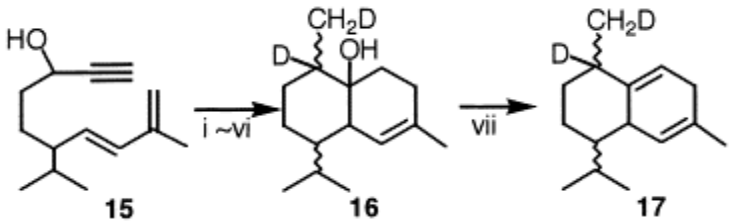

There were several steps taken in the biotransformation of cubenene and calamenene in 28 day old H. planus cultures. The treated cultures were first incubated and stirred under light for 12 hours. The solution was then centrifuged and the cell was washed with water and ether, then the cells were removed with methanol and partitioned with n-pentane.

Table 1. Biotransformation of cubenene (50 μg) in the suspension culturedcells of *H. planus*. Values are expressed as μg per μl culture medium (0.04 g fr. wt.) and represent the mean±S.D. (*n*=2)

Incubation time (h)	**Cubenene (μg/μl)**	**7-Hydroxycalamenene (μg/μl)**	**Calamenene (μg/μl)**
0	0.46±0.09	0.12±0.02	0.68±0.05
12	2.20±0.20	0.35±0.08	1.20±0.10
(12–0)	1.74	0.23	0.52
12[a] (without substrate)	0.40±0.02	0.14±0.01	0.60±0.03

a

Significant increase (>0.1 μg/0.04 g fr.wt.) in amounts of cubenene, calamenene and 7-hydroxycalamenene was not observed during 12-h incubation without precursors.

Table 1 provides the results of the biotransformation of cubenene in the suspension cultured cells of H. planus. When the cells were incubated for twelve hours with 50 ug/ml of cubenene the values from the table indicates an increase in the amount of 7-hydroxycalamenene to 0.35(+/-) 0.08 from 0.14(+/-) 0.01 when no substrate is used. The amount of calamenene also shows a significant increase when this substrate is used to

1.20(+/-) 0.10 which is almost triple the value when there is no substrate used. The results in table 2 provides evidence that when incubated with calamenene, the amount of 7-hydroxycalamenene did not increase. This data suggest that the 7-hydroxycalamenene results from cubenene and calamenene is either absorbed on the cell or not removed when washed with ether. The mass spectra of 7-hydroxycalamenene with (2H2)-cubenene and (2H6)-calamenene reveals a base ion signal at 177 m/z, which is characteristic of two (2H) atoms connected to the dihydronapthalene ring. When calamenene was the substrate there was no base ion peak close to this. The findings in this study suggest that 7-hydroxycalamenene biosynthesis involves (2H2)-cubenene and not (2H6)-calamenene.

Article # 10

Title: Synthesis and reactivity of (l-g2:g2-peroxo)dicopper(II) complexes with dinucleating ligands: Hydroxylation of xylyl linker with a NIH shift

Summary:

The synthesis and reactivity of dicopper (II) compounds with dinucleating ligands connected to xylyl linkers are studied. It has been noted that copper (I) complexes react with dioxygen to form intra and intermolecular dicopper (II) compounds. In previous studies the dicopper (II) complexes have been shown to cause hydroxylation of the xylyl linker ligands and intermolecular arene hydroxylations have proved that phenolates are hydroxylated by the dicopper (II) complex. In this study the authors produced dinucleating ligands and the dinuclear copper (I) complexes for future studies involving these compounds and their mechanisms. There are several methods used in this study including: NMR spectroscopy, FT-IR spectroscopy, Diode Array spectrometer, and Mass

spectroscopy. The results are discussed in terms of the synthesis and characterization of the copper (I) complexes, and the spectroscopic characterization and self decomposition of Cu (II) 2 complexes.In new dinuclear ligands namely Me2–L–Me and H–L–F and their dinuclear copper (I) complexes [Cu2(Me2–L–Me)]2+ and [Cu2(H–L–F)]2+ are used to examine the physicochemical properties of a copper (II) complex. The decomposition of 1-dioxygen resulted in hydroxylation of the xylyl linker of Me2–L– Me with a 1, 2-migration of the methyl group. The formation of intramolecular and intermolecular species are highly dependent on the concentration of complex, and the nature of the side arm of the dinucleating ligand. Introduction of a fluoro group into the xylyl linker tends to produce ntermolecular (l-g2:g2-peroxo)-Cu (II) 2 species. Because the fluoro and methyl groups in the bridging xylyl linkers are big, the intensity of the LMCT transition decreases as the transition energy decreases.

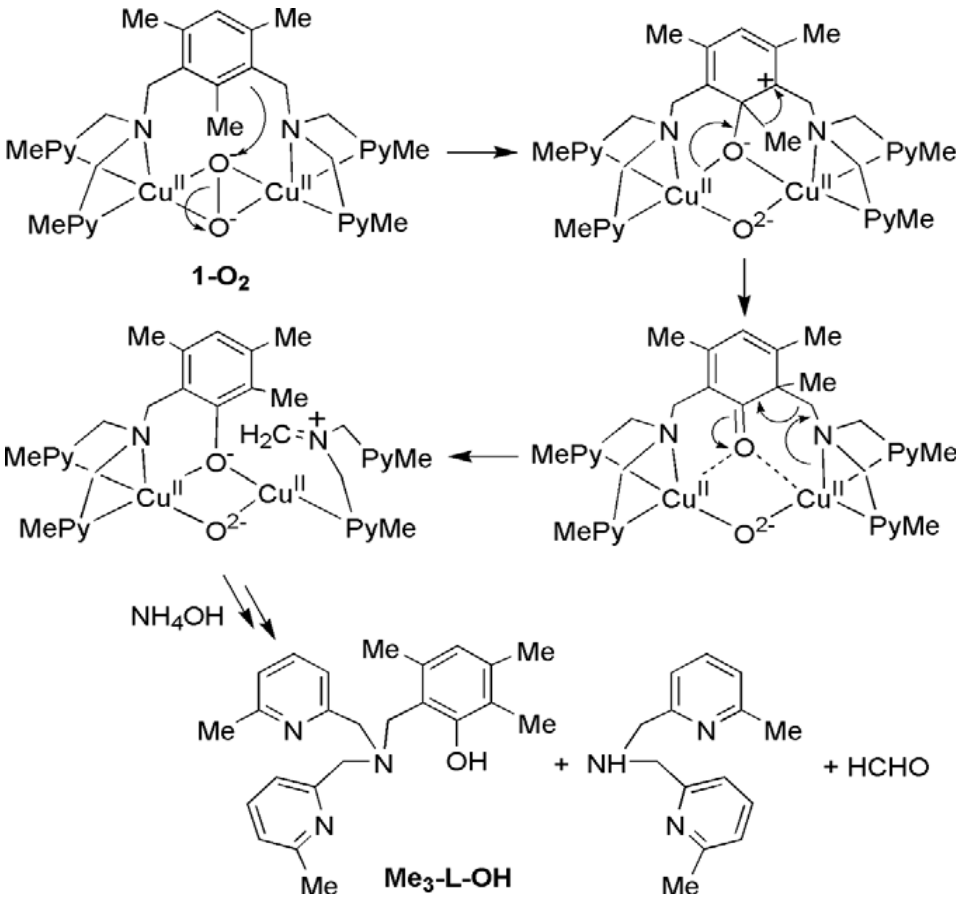

Sheme #3 shows an oxidation pathway of [Cu2(o2)(Me2-L-Me)]2+ and (1-O2) with 1,2-methyl migration indicating that Me2–L–Me ligand is hydroxylated at the 2-position of the xylyl linker. In this paper, the authors successfully synthesize dicopper(I) complexes with dinucleating ligands having a xylyl linker, [Cu2(X–L– R)]2+ (1 and 2), that generate (l-g2:g2-peroxo)Cu(II)2 and, [Cu2(O2)(X–L–R)]2+ (1-O2 and 2-O2) compounds. The results reveal that at high concentration the copper complexes 1 and 2 produce intermolecular (lg 2:g2-peroxo) Cu (II)2, while at low concentrations the complexes produce intramolecular copper (II) species. Hydroxylation of the 2 position of the linker with a NIH shift of the methyl group stems from decomposition of the dioxygen compound. This is indicative of an electrophilic aromatic substitution that involves a

carbocation intermediate. In this study the authors use the copper (I) reaction sites to investigate these compounds using a synthetic model to probe there activity.

Article: #11

Title: NIH Shift in the Hydroxylation of Aromatic Compounds by the Oxide Intermediate? Ammonia-Oxidizing Bacterium Nitrosomonas europaea. Evidence against an Arene Oxide intermediate

Summary:

In earlier studies arene oxides were found to spontaneously rearrange into a phenol, radical, carbocation and ketone. In this study aromatic compounds are used as substrates and there products are examined and reported. Monooxygenase enzymes are a class of enzymes that catalyzes the reduction of a single oxygen atom from molecular oxygen in the substrate to water and also the addition of the second oxygen atom in molecular oxygen in the substrate to water. In previous studies several intermediates have been projected, arene oxides are said to spontaneously rearrange into a phenol compound that can react with reagents to form radicals, carbocations and ketones. The methods used in this article include gas chromatography which is used for the determination of the formation of phenols. GC/MS is used for the identification of deuterium content of the substrate and the phenolic product measurements. NMR for identification of phenolic products, TLC for separation and purity of products, and colorimetric assay is used for identification. The results are discussed in terms of the identification of products, values of the NIH shift for the deuterium or hydrogen shifts and there retention, and the kinetic isotope effects. Table 1 gives the results of the products formed from the hydroxylation

of aromatic substrates by AMO. The recovery of the substrate and product were high although the values were dependent on the concentration of the substrate and the volatility of the substrate used. The aromatic compounds in the presence of ammonia, stimulated the compounds hydroxylation reaction. The aromatic compounds inhibited the production of nitrite from ammonia. Also the transforming of anisole, fluorobenzene, naphthalene, and benzonitrile by AMO was shown in this study first. The beginning concentration of substrate resulted in the greatest amount of phenolic product. Aromatic hydroxylation with para, or ortho directed substituents on the ring, resulted in para phenols as the main product of this hydroxylation reaction. When the hydroxylation of aromatic compounds with meta directed substituents, the results provide evidence of meta and para phenols. The meta phenol is the main product in the nitrobenzene hydroxylation, and the hydroxylation fluorobenzene the only product was para-phenol. Ethylbenzene, anisole and toluene all involved a nonaromatic hydroxylation mechanism. Toluene hydroxylation produced benzyl alcohol, and the oxidation of ethylbenezene produced three hydroxylation products; 1 and 2-phenylethanol and para-ethylphenol. From the NMR data obtained the results suggest the retained deuterium is at the 2 and 6 position of the 4-bromo and 4-chlorophenol compounds, and it was also retained at the 6 position for 3-nitrophenol. In this study some of the hydroxylations did not take place at the site adjacent to deuterium, in these mechanisms all deuterium is retained. The product distribution of deuterium in the hydroxylation products proves no different for deuterated or nondeuterated substrates. There were no visible effects on the distribution of the products when the aryl ring was labeled with deuterium. Fluorobenzene and bromobenzene compounds showed no apparent isotopic. The para dueterated phenols

showed a broad range for there NIH values ranging from 0 to 83%and the meta phenols values show a slight increase to 72 to 95%. The meta phenols values were in the same range NIH shift values from 59 to 79%. Deuterium retention in ortho-fluorobenzenes was 35%, because it is so low the value of retention could not be determined in this paper. The results of the meta phenols retention of deuterium from ortho deuterated nitro and fluorobenzene was fairly high in the range of 90-96% when.

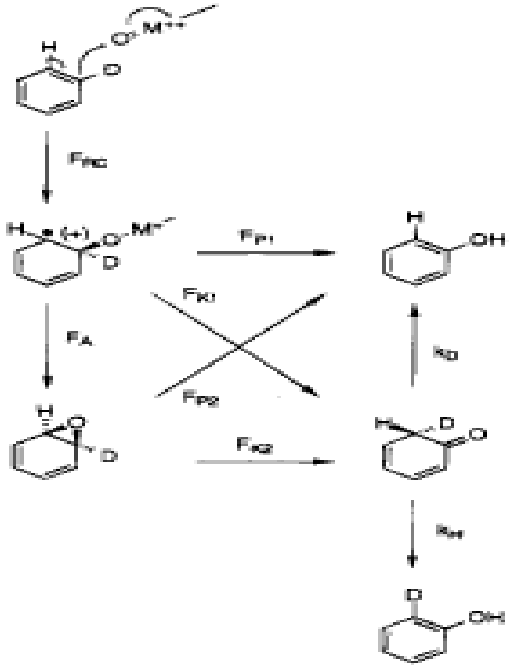

Figure #3 shows possible reaction pathways involving cationic and radical intermediates that arise due to aromatic substrates reacting with activated oxygen. If the intermediate breaks down it could, form a phenol with no labeled deuterium, a ketone that can enolize and form phenol with, retention or loss of deuterium, an arene oxide that can undergo tautomerization to get a phenol with loss of deuterium or a ketone intermediate which can enolize to form phenol with loss or retention of deuterium. In this study the authors prove the hydroxylation of an aromatic ring by AMO to the corresponding phenolic products

involves electrophilic addition. There was no evidence that suggest an arene oxide intermediate in any of the substrates examined. The same was true for the hydroxylation of nitrobenzene to meta-nitrophenol. Due to no ortho phenolic products proves that arene oxides do not exist in this reaction. Although, no evidence exist for arene oxides it should not be ruled out of all substrates examined because there are possibilities for an arene oxide to form.

Nitrobenzene oxidation to meta-phenols has lower deuterium retention values when the site for hydroxylation is deuterated, rather than when the retention is at other positions. A direct loss mechanism shown in scheme 3, could be the cause for the low NIH shift values observed in this study, but there is no direct evidence of these findings. The findings observed in this study suggest that the formation of phenolic products prove evidence of an electrophilic addition reaction coupled with a shift of hydrogen or deuterium. A ketone intermediate common to all the reactions, seems apparent in these reactions due to the NIH shifts values, and the improbable formation of an arene oxide and the loss of deuterium during the hydroxylation of nitrobenzene. The enzyme used has a direct effect on the site where hydroxylation occurs and the degree of the NIH shift during hydroxylation of ring substrates. These results are suggestive of a radical or carbocation formation. And further studies could use the techniques in this study to probe these mechanisms.

Article: #12

Title: [1, 2]-Aryl migration in the synthesis of substituted indoles: scope, mechanism, and high throughput experimentation

Authors: Tao Pei, David M. Tellers, Eric C. Streckfuss, Cheng-yi Chen, Ian W. Davies

Date: 7 November 2008

Journal: Tetrahedron

Summary:

This study examines the (1, 2)-Aryl (NIH) shift in the synthesis of substituted indoles. In past studies, indole synthesis is proven to be very limited making the need for an efficient synthesis method of indole important. Indole is present in many biologically active compounds, and recent developments reporting effecient synthesis of substituted indoles is underway. The authors in this study develop an efficient regioselective synthesis of indole using a wide variety of organometallic reagents.

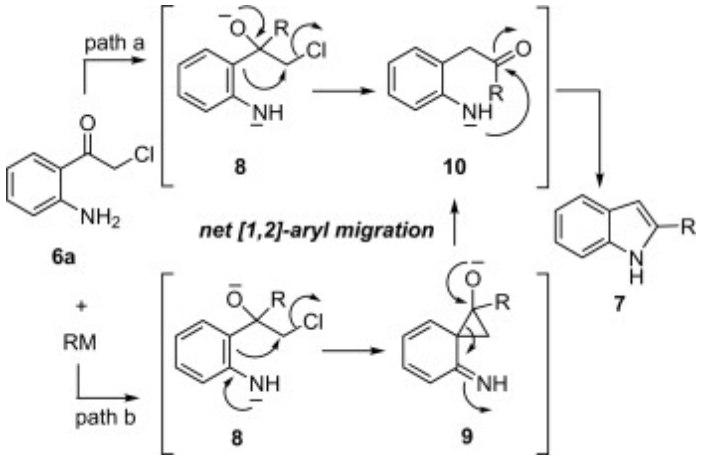

Figure #1 presents a mechanism for the synthesis of 2-substituted indole that starts with the organometallic nucleophile adding to the chloroketone to form the resultant tertiary alkoxide. This tertiary alkoxide undergoes a NIH aryl shift that results in a ketone(10). Dehydration and cyclization following the formation of the ketone, provides the 2 substituted indole. The nitrogen component on aniline affords the NIH aryl shift by one of two routes, either by conventional migration or thru the bicyclic anion intermediate

route. The first method describes the reaction depicted in scheme 3 below, where the ketone(6a) and dianion(11) react allowing the aniline group to migration to produce the product (13) with a 65% yield. The formation of intermediate (12), results in two possible aniline derivatives that participate in the NIH shift of the aryl group.

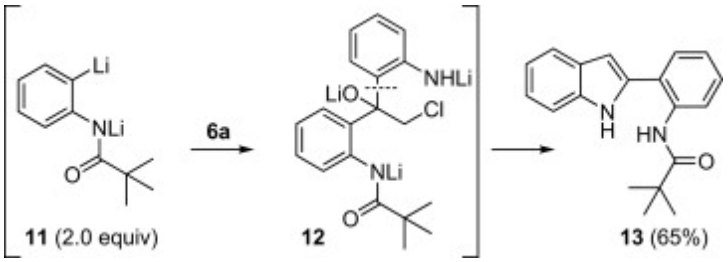

The second method is shown in scheme 4 produces a slightly higher yield of 69% for the product. This reaction involves treatment of the ketone (3) with NaBD4 and dioxane/H2Osolution to get the labeled alcohol (14) that after treatment with PrMgCl/THF provides formation of 2-D-7-chloroindole (15).

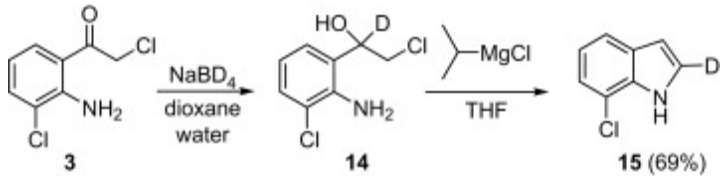

The authors used a variety of organometallic reagents to further examine the synthesis of 2-substituted indoles from the ketone(3) and the results are summarized in table 1. The first two complexes provide very high yields of 89% and 86% for the 2-substituted indole products, while the 3rd and 4th indoles were treated with the organolithium reagents show slightly lower yields of 76% and 70%. The indoles in 6 through 9 produced fairly high yields with the addition of an aryl or heteroaryl to the ketone(3). The yield of products in these four indoles is 91% for (5g), 78% for (5h), 76% for (5i), and 72% for (5j). The last two complexes employed a direct synthesis that stem from the alkynyl magnesium compound with lower yields of 54% and 55%. Table 2 provides the products

when other substituted ketones are used, namely (6). The yeilds of the products vary with the different ketones used. The highest yeild is observed in (7g) with a 91% yield of the product, (7a) has the second highest yield of 76%, and (7f) follows with a yield of 75%. The complexes remaining (7b to 7e) yields are between 52% and 68%, these are slightly smaller than the other three complexes. The region selective synthesis of 2, 3-disubstituted indoles was examined using the ketone(16) shown in scheme 5. (17a) gives the highest yield of product 93% when in toluene and only 67% when in THF, and (17b) in toluene produced yields of 80%. The final synthesis was performed on a library of indoles to expand the scope of practice and to synthesize a variety of substrates for further evaluation. This synthesis was performed with THF/toluene as the solvent in a 96-well plate, this allowed the experimenters the opportunity to make a number of indole derivatives using different reagents at one time. HPLC was used to purify and tract the transformation of the compounds while high resolution mass spectroscopy was used in the identification of the resultant products. There were 62 indoles recovered with a 90% or more purity, and the other 34 indoles had yields to low for isolation. In conclusion this study has provided the researchers with new ways to synthesize indoles involved in 1, 2-aryl migration. This synthesis is regioselective due to the addition of the variety of substituents to the indoles 2C position. The new methods employed in this study can be utilized by others along with the previous synthesis methods in future studies. All of the reagents and solvents obtained from commercial suppliers were used without purification or drying and all reactions were conducted in standard RB-flasks under a nitrogen atmosphere. NMR spectra were obtained on Burker spectrometer and flash column chromatography was performed, eluting with mixtures of hexanes and ethyl acetate.

HPLC was performed on an Agilent and a modified procedure of Sugasawa reaction was used to react anilines with nitriles. Aniline and chloroacetonitrile were added sequentially to a mixture of $AlCl_3$ pellets and BCl_3 solution with dichloromethane cooled in ice bath. Then the cloudy solution was stirred for 1 1/2hours at room temperature before heating for 12 hours. The reaction mixture was then cooled in ice bath, quenched with HCl heated, cooled, and extracted with dichloromethane. The combined organic layers were dried over $MgSO_4$, concentrated, and chromatographed to afford corresponding 2-chloroethanone. To a solution of alpha-chloro acetophenone either toluene or THF was added dropwise to a solution of RMgX or RLi. The reaction was stirred in cold bath for before removal of the bath. The mixture was then quenched with diluted aqueous NH_4Cl, extracted with MTBE, washed with brine, and dried over $MgSO_4$. After concentration, the crude residue was chromatographed to give the desired indole.

To a solution of 1-(2-amino-3-chlorophenyl)-2-chloroethanone in 1,4-dioxane and water then $NaBD_4$ was added, aged for one hour, quenched with saturated NH_4Cl, extracted with MTBE, washed with brine, and dried over $MgSO_4$. After concentration, the crude residue was chromatographed to give the alcohol in 14. A THF stock solution of each ketone was prepared in THF was transferred with a multichannel pipetter to 1mL vials containing stirbars in the appropriate row of the aluminum 96-well plate. The THF was removed via evaporation in a centrifuge and the 96-well plate was brought into an inert atmosphere glovebox, placed on a tumble stirrer equipped to a circulating cooler, and THF/toluene was added to each well. The plate was cooled and Grignard reagent was added in four portions through a multichannel pipetter over a 45minute period. After addition, the reactions were warmed for over one hour. Then the solutions were cooled

and diluted with aqueous ammonium chloride and MTBE and were added to each vial. After warming to room temperature, the 96-well plate was removed from the glovebox and the organic layer was separated and washed with brine. The conversion, purity, and identity were examined using a portion of each solution, and then diluted, and analyzed by HPLC. The remaining solution was concentrated under reduced pressure and redissolved in DMSO.

Article: #13

Title: 1, 2-Acyl group migration in the oxidative free radical reaction of 2-substituted-1, 4-quinones

Summary:

Quinone is an important entity in many natural products and biologically active compounds, thus proving its importance in the environment. The synthesis of this compound and its derivatives would afford the researchers the ability to gain insight into quinone and its mechanism. This study examines the oxidative free radical mechanism of 1, 4-quinone derivatives that employs a NIH shift of the acyl group. The researchers report there findings in terms of the spirolactam that results from the 1, 4-quinone derivatives and the NIH shift of the acyl group. The indole rings of indoloquinones provide a common building block to the naturally occuring quinones, and synthesis of these rings would prove beneficial in studies of these complexes. The authors began there research with the manganese (III) oxidative free radical mechanism depicted in figure #1.

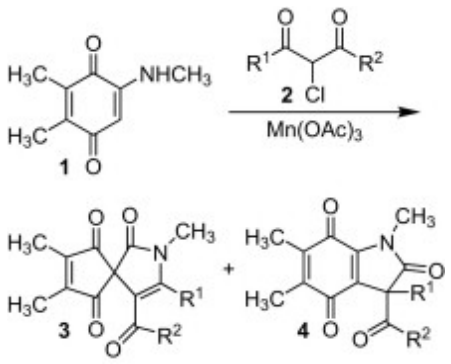

The 1, 4-benzoquinone (1) reacts with the manganese(III)/acetic acid and ethyl 2-chloroacetoacetate(2), the spirolactam(3) is the product. This reaction did not produce any indole diones or tiones as a result of the mechanism. The spirolactum that results from this reaction could have resulted from the mechanism dipicted in scheme 1.

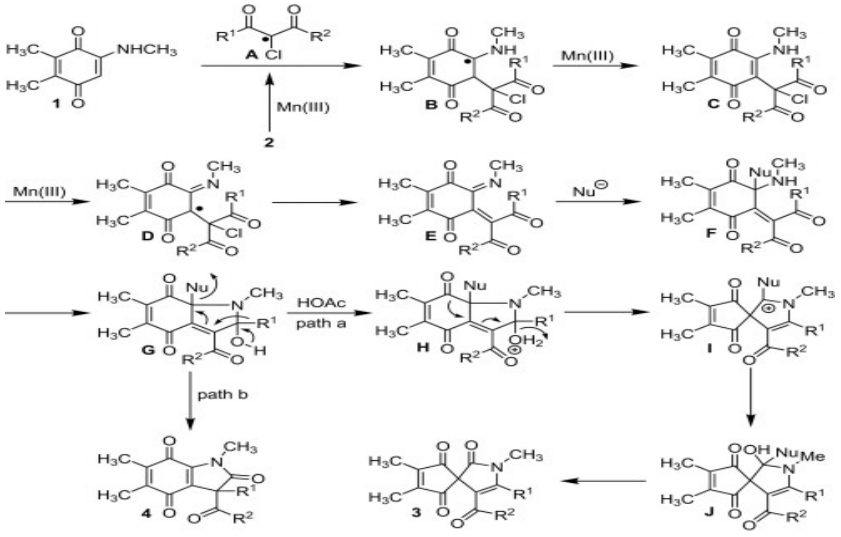

This mechanism begins with oxidation of ethyl 2-chloroacetate with the manganese (III) acetate to form a radical. This radical undergoes an intermolecular addition to the quinone ring and when treated with the manganese (III) further oxidation produces C-a. Upon oxidation of the C-a compound with the manganese (III), the loss of chlorine produced the imine complex in E-a. This complex is then converted to G-a once it reacts with the nucleophile acetate ion, which provides a nucleophilic addition to the ring and

cyclization. Finally, there is a protontion of G-a that is followed by an NIH acyl shift and hydolysis that provides the spirolactum complex. The yield of the spirolactum is only (39%) for the compound generated in pathway (a), there were also small yields of this compound when other beta ketoesters were used.

Table #1 provides the product yield in percent when other metal salts were used in the free radical reactions. When potassium cyanide and sodium chloride are used the yields of spirolactum are comparitively higher than when just the manganese (III) acetate is used. The 1, 4-quinone in acetic acid can react with the manganese (III) acetate and the methyl-2-chloro-isobutyrylacetate, gives the 4a complex that stems from the NIH alkyl shift of the isopropyl group in G-e. The indole-2, 4, 7-trione yield in this reaction is small as seen in table#1, which shows a 30% yeild of the product. Scheme 2 shows the reaction with 1, 4-naphthoquinone (5) with (2a) formed the spirolactum(6f) with a 40% yield. The spirolactum(6) can form from other reactions involving the beta enamino carbonyl(8) and the 2-hydroxy-1,4-napthoquinone(7). Table 2 provides the product yields of the spirolactums that form from the reactions with the beta enamino carbonyl and the 2-hydroxy-1, 4-napthoquinone. The first four entries provide evidence of fairly higher yields when the beta enamino ketones were used than when the beta enamino ester is used. The cerium(IV) salt is used with out the acid to probe an alternative method that may improve the yield of the spirolactum product. When the solvent (TBACN) is used in the reaction of (7) with (8a) it gave the resultant (6a) in a 66% yield. The authors used a methanol solvent and a chloroform solvent that also produced even higher yields of the spirolactum 83% and 91%, respectively. The other seven compounds using different beta enamino carbonyls gave high yeilds of 6a. The resultant higher yields of spirolactum

provide evidence that both the beta enamino ketones and esters can be used to produce spirolactum. The results of this study prove that the reaction of the 2-hydroxy-1, 4-naphthoquinone with beta enamino carbonyl with the (TBACN), produces the spirolactum(6) in high yeilds, although the combination of TBACN/CHCl3 solvent provides the best reaction conditions for the formation of the complex. There was also proof of an imine radicals formation when the beta enamino carbonyl is oxidized by the two salts, and formation of a radical from the oxidation of the alpha-chloro-beta-ketoester adds to the double bond of the 1,4-benzoquinone. The manganese (III) free radical reactions provide an effective method for the formation of spirolactum and the 2,4,7-trione. In future research the authors should employ a variety of solvents to explore the mechanisms of the acyl migration decribed in this study. There were no corrections performed for the melting points. Infrared spectra were taken and H and C NMR spectra were recorded. Chemical shifts are reported in parts per million relative to TMS as internal reference and elemental analyses were performed. X-ray diffraction structure analyses were performed and structure analysis was done on a personal computer. Analytical thin-layer chromatography was employed and visualized by UV spectroscopy. The reaction mixture was purified by column chromatography and the starting 5,6-dimethyl-2-(methylamino)-1,4-benzoquinone, 2-(methylamino)-1,4-naphthoquinone and alpha-chloro-beta-ketoesters were synthesized according to literature procedures. A mixture of 5, 6-dimethyl-2-(methylamino)-1, 4-benzoquinone, ethyl 2-chloroacetoacetate and Mn(OAc)3 in acetic acid was stirred for one hour. Then this mixture was diluted with ethyl acetate, washed with saturated aqueous sodium bisulfite, water, saturated aqueous sodium bicarbonate and dried (Na_2SO_4). The solvent was evaporated under reduced

pressure and the crude product was purified by column chromatography using ethyl acetate/hexane as the eluent, followed by crystallization (ethyl acetate/hexane). A solution of 2-hydroxy-1, 4-naphthoquinone, 4-methylamino-3-penten-2-one aqueous methylamine and TBACN in chloroform was stirred for 30minutes. Then the remaining crude product was purified by column chromatography using ethyl acetate/hexane for the eluent, followed by crystallization (ethyl acetate/hexane).

Article: #14

Title: Intramolecular Oxygen Atom Transfer from a Carbonyl Oxide Moiety to a Methoxyvinyl Group

Authors: Norinaga Nakamura, Masatomo Nojima, and Shigekazu Kusabayashi

Date: February 18, 1986

Journal:

Summary:

The authors provide sufficient evidence that an electron rich intermediate can be oxidized causing an intramolecular transfer of the oxygen atom to the methoxyvinyl group. There are other studies on the carbonyl oxide intermediates that prove transfer of the oxygen atom in oxygenation of electron deficient olefins. The experimenters tried a different approach to prove the importance of these intermediates in oxidation reactions. These intermediates act as nucleophilic oxygen transfer reagents in oxygenation and others have proved the transfer of an oxygen atom from these intermediates allows them to be used as models for some reactions catalyzed by monooxygenase enzymes. The first scheme

describes the reaction of the diene #1 to form the keto ester #2 when treated with 1mol and 2mol equiv. of ozone in tetrachloride. When the diene (1) reacts with the ozone it attaches to the double bond that has the phenyl and methoxy molecules attached to the ends of the double bond as seen in 3. The structure of the ozonide in 3 could break down to form the carbonyl oxide intermediate seen in the fourth figure. The keto ester in the structure of 2 is the result of this reaction if the intermediate in 4 undergoes an intramolecular oxygen transfer along with a NIH shift of the hydride ion. This route produced a good yeilds of 62% for the isolated ketoester, and 35% of the starting materials.

Scheme 1

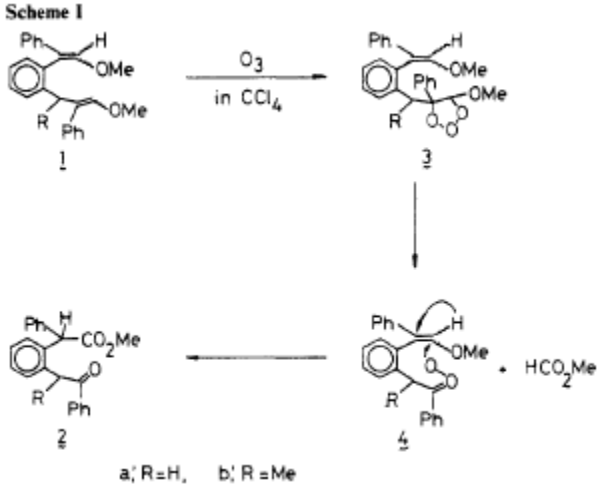

There are other possible routes, through direct intramolceular oxygen transfer from ozonide, which could result in repetition of the prior sequencing mentioned. The results of the product consist of (36%) of the beginning product, 6% diketone, 12% keto ester, and 24% keto olefin. These yeilds provide evidence that an intramolecular oxygen transfer mechanism from the intermediate in 4 occurred, due to the decrease in the keto ester from 62% to 12% and the formation of the diketone and the keto olefin that are not

present in the first reactions yeild.

Scheme (II)

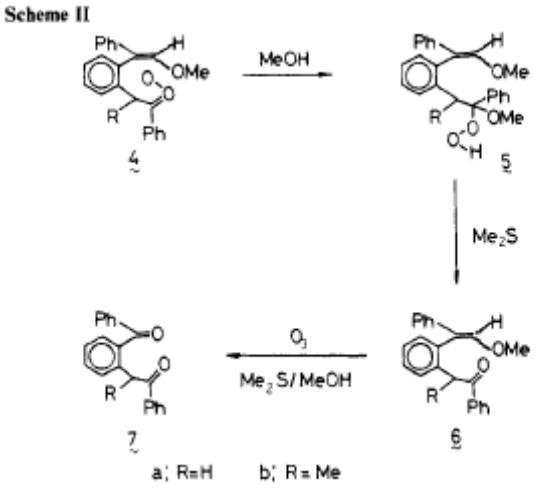

Scheme II
MeOH
Me2S
O3
Me2S/MeOH
a; R=H
b; R=Me

The reaction in scheme II provides an explanation of the intramolecular transfer mechanism from the carbonyl oxide intermediate. When carbonyl oxide intermediate 4 is treated with methanol the hydroperoxide 5 results. Treatment of the hydroperoxide 5 with dimethyl sulfide results in the keto olefin 6. When the keto olefin is reacted with ozone and dimethysufide/methanol the diketone7 is the resultant compound. Previous data suggest carbonyl oxides are poor reagents for epoxidation of olefins, but the data here

suggest that in some desirable instances, the oxygen transfer process proves to be an efficient route. The results show that intramolecular oxygen transfer from carbonyl oxide intermediates offers an efficient alternative to the process. The intermolecular transfer of the oxygen atom proves to be a slow process that employs other reactions that have precedence over the actual oxygen transfer. In this study the authors conclude that the epoxidation of electron rich olefins is possible. In future studies the authors can further there investigation of electron rich compounds to broaden there scope.

References:

1.) Patrick J. Hillas and Paul F. Fitzpatrick, A Mechanism for Hydroxylation by Tyrosine Hydroxylase Based on Partitioning of Substituted Phenylalanines Biochemistry, 1996,35, 6969-6975

2.) Koichi Haraguchi, Yoshihisa Kato, Ryohei Kimura, and Yoshito Masuda Daiich Tamagawa-Cho, Minami-Ku Fukuoka Yada, Shizuoka, Hydroxylation and Methylthiolation of Mono-Ortho-Substituted Polychlorinated Biphenyls in Rats: Identification of Metabolites with Tissue Affinity, Toxicology, 1998, 11, 1508-1515

3.) Graham R. Moran, Robert S. Phillips, and Paul F. Fitzpatrick, Influence of Steric Bulk and Electrostatics on the Hydroxylation Regiospecificity of Tryptophan Hydroxylase:

Characterization of Methyltryptophans and Azatryptophans as Substrates Chem. Res. Toxicology, 1999, 38, 16283-16289

4.) Graham R. Moran, Agnes Derecskei-Kovacs, Patrick J. Hillas, and Paul F. Fitzpatrick, On the Catalytic Mechanism of Tryptophan Hydroxylase, Journal of the American Chemical Society, 2000, 122, 4535-4541

5.) WOLFGANG ENGEL, Deutsche Forschungsanstalt fu¨r Lebensmittelchemie, Lichtenbergstrasse, Detection of a “Nonaromatic” NIH Shift during In Vivo Metabolism of the Monoterpene Carvone in Humans, Journal of Agricultural and Food Chemistry 2002,50,1686-1694

6.) Hiromi Ohi, Yoshimitsu Tachi, and Shinobu Itoh, Sumiyoshi-ku, Modeling the Mononuclear, Dinuclear, and Trinuclear Copper(I) Reaction Centers of Copper Proteins Using Pyridylalkylamine Ligands Connected to 1,3,5-Triethylbenzene Spacer, Inorganic Chemistry, 2006, 45,10825-10835

7.) Michael P. Jensen, Steven J. Lange, Mark P. Mehn, Emily L. Que, and Lawrence Que, Jr., Biomimetic Aryl Hydroxylation Derived from Alkyl Hydroperoxide at a Nonheme Iron Center. Evidence for a FeIVdO Oxidant, Journal of the American Chemical Society, 2003, 125, 2113-2128

8.) William E. Robinson Kenneth Kustin, Kimberly Matulef, David L. Parry, Xiaoying He and Evelyn K. Ryan 14C- and 3H-Tyrosine Incorporation into Ascidia ceratodes Tunichrome In Vivo, Comp. Biochemistry. Physiology, 1996,115, 475-481

9.) Makoto Hashimoto, Reiko Hozumi, Masateru Yamamoto, Kensuke Nabeta, Biotransformation of cubenene to 7-hydroxycalamenene in cultured cells of the liverwort, Heteroscyphus planus, Phytochemistry 1999, 51, 389-394

10.) Takahiro Matsumoto, Hideki Furutachi , Shigenori Nagatomo, Takehiko Tosha, Shuhei Fujinami, Teizo Kitagawa, Masatatsu Suzuki Kakuma-machi, Myodaiji, Okazaki Synthesis and reactivity of (l-g2:g2-peroxo)dicopper(II) complexes with dinucleating ligands: Hydroxylation of xylyl linker with a NIH shift, Journal of Organometallic Chemistry, 2007, 692, 111-121

11.) Todd Vannellit and Alan B. Hooper, NIH Shift in the Hydroxylation of Aromatic Compounds by the Oxide Intermediate? Ammonia-Oxidizing Bacterium Nitrosomonas europaea Evidence against an Arene Oxide intermediate, Biochemistry, 1995, 34, 11743-11749

12.) Tao Pei, David M. Tellers, Eric C. Streckfuss, Cheng-yi Chen, Ian W. Davies [1, 2]-Aryl migration in the synthesis of substituted indoles: scope, mechanism, and high throughput experimentation, Tetrahedron, 2009, 65, 3285-3291

13.) An-I Tsai, Che-Ping Chuang, 1, 2-Acyl group migration in the oxidative free radical reaction of 2-substituted-1, 4-quinones,Tetrahedron, 2008,64,5098-5102

14.) Norinaga Nakamura, Masatomo Nojima, and Shigekazu Kusabayashi, Intramolecular Oxygen Atom Transfer from a Carbonyl Oxide Moiety to a Methoxyvinyl Group, Journal of the American Chemical Society, 1986, 108, 4671-4672

15.) Kumar S., Murray R. W., Carbonyl Oxide Chemistry. The NIH Shift, Journal of the American Chemical Society, 1984, 106, 1040-1045

16) Brown H. William, Foote S. Christopher, Iverson L. Brent, Organic Chemistry, 4th ed; Brookes/Cole, 2005

17.) Chemistry Dictionary Online, www.chemicaldictionary.org

18.) Wikipedia, The free online encyclopedia www.wikipedia.org